Molecular Neurobiology (2019) 56:5815–5834
https://doi.org/10.1007/s12035-019-1475-8

Mechanisms Associated with Type 2 Diabetes as a Risk Factor for Alzheimer-Related Pathology

Men Su[1,2] · Kambiz Naderi[1] · Nathalie Samson[1] · Ihsen Youssef[3] · Livia Fülöp[4] · Zsolt Bozso[4] · Serge Laroche[1] · Benoit Delatour[3] · Sabrina Davis[1]

Received: 11 September 2018 / Accepted: 10 January 2019 / Published online: 25 January 2019

Abstract

Current evidence suggests dementia and pathology in Alzheimer's Disease (AD) are both dependent and independent of amyloid processing and can be induced by multiple 'hits' on vital neuronal functions. Type 2 diabetes (T2D) poses the most important risk factor for developing AD after ageing and dysfunctional IR/PI3K/Akt signalling is a major contributor in both diseases. We developed a model of T2D, coupling subdiabetogenic doses of streptozotocin (STZ) with a human junk food (HJF) diet to more closely mimic the human condition. Over 35 weeks, this induced classic signs of T2D (hyperglycemia and insulin dysfunction) and a modest, but stable deficit in spatial recognition memory, with very little long-term modification of proteins in or associated with IR/PI3K/Akt signalling in CA1 of the hippocampus. Intracerebroventricular infusion of soluble amyloid beta 42 (Aβ42) to mimic the early preclinical rise in Aβ alone induced a more severe, but short-lasting deficits in memory and deregulation of proteins. Infusion of Aβ on the T2D phenotype exacerbated and prolonged the memory deficits over approximately 4 months, and induced more severe aberrant regulation of proteins associated with autophagy, inflammation and glucose uptake from the periphery. A mild form of environmental enrichment transiently rescued memory deficits and could reverse the regulation of some, but not all protein changes. Together, these data identify mechanisms by which T2D could create a modest dysfunctional neuronal milieu via multiple and parallel inputs that permits the development of pathological events identified in AD and memory deficits when Aβ levels are transiently effective in the brain.

Keywords Type 2 diabetes · Alzheimer's disease · Amyloid beta · PI3K-Akt signalling · Insulin · Human junk food · CA1 · Object recognition · Environment enrichment

Introduction

Until more recently, much of the research into how pathology in Alzheimer's disease (AD) induces dementia has focussed on the amyloid plaque, to the relative neglect of non-amyloid specific pathologies associated with the disease. However, the past decade has witnessed a paradigm shift away from the hard core amyloid plaque as the major pathological mechanism inducing the disease and ensuing dementia to the role of soluble, toxic species of preaggregated amyloid and non-specific pathologies [1, 2]. The main evidence supporting this is treatments in clinical trials that remove plaques do not result in improvement or slowing of the dementia [3], and imaging studies suggesting amyloid load is an age-related phenomenon that does not necessarily lead to dementia [4, 5]. Both epidemiological and experimental evidence have identified a number of dysfunctional/pathological events in AD, that are not specific to AD, that include dysfunction in energy

Electronic supplementary material The online version of this article (https://doi.org/10.1007/s12035-019-1475-8) contains supplementary material, which is available to authorized users.

✉ Sabrina Davis
Sabrina.davis@u-psud.fr

[1] Département Cognition & Comportement, Institut de Neurosciences Paris-Saclay (Neuro-PSI) CNRS UMR 9197, Université Paris Sud, Bat. 446, 91405 Orsay, France

[2] Present address: Division of Episomal Persistent DNA in Cancer and Chronic disease, German Cancer Research Centre (DKFZ), 69120 Heidelberg, Germany

[3] Institut du Cerveau et de la Moelle épinière, INSERM, CNRS, Sorbonne Universites, ICM, 75013 Paris, France

[4] Department of Medical Chemistry, University of Szeged, Dómtér 8., Szeged 6720, Hungary

regulation, supply of nutrients, oxidative/ER stress, inflammation, mitogenic abnormalities, synaptic failure, autophagy and disruption of the blood brain barrier and neurovasculature [6–14].

A key question is whether these dysfunctions are directly linked with the classic AD pathology in terms of being a cause or consequence of amyloid pathology, or whether they are independent pathologies occurring in parallel with amyloid pathology. Whether causal or independent, it suggests that these dysfunctional events may constitute a multiple 'attack' on the brain, and the question becomes how they are induced. Many of these dysfunctional events are associated with known metabolic risk factors for developing AD that develop slowly over time.

Ageing is the major risk factor for developing AD, however, following that type 2 diabetes (T2D), poses the greatest known risk; epidemiological studies show a large percentage of people with T2D go on to develop AD [15] and diabetic patients show similar cognitive deficits to those at early stage AD [16]. Adult T2D is characterised by peripheral hyperglycemia, dysfunctional insulin signalling and chronic low-grade inflammation and begins to manifest the symptoms in mid life, a time that coincides with the early increase in soluble Aβ40/42 in the brains of human subjects predicted to develop AD [17]. However, as AD, T2D is a multifactorial disease and subject to risk factors, most notably obesity [18] that is highly linked with the development of hyperinsulinemia [19] and develops slowly over time.

Both diseases share common pathologies albeit they have been identified in the periphery with T2D and in the brain with AD. These include an increase in inflammation, dysregulation of glucose and insulin signalling and these are mediated, at least in part, via IR/PI3K/Akt signalling [20, 21]. Although it has been suggested that T2D pathologies can promote early neurodegenerative processes, the mechanisms by which this occurs are complex and poorly understood [see 22]. One possibility is that peripheral hyperinsulinemia and hyperglycemia associated with T2D impairs the uptake of insulin and glucose across the blood brain barrier (BBB) [23] to induce dysfunctional insulin signalling in the brain, and chronic low-grade inflammation may impact the BBB to allow inflammatory molecules to pass through.

To date, numerous studies have shown links between pathologies associated T2D and AD using different approaches. For example, dysfunction regulation of the IR/PI3K/Akt signalling pathway has been shown in postmortem brains of patients with AD [24–26]; development of AD pathology observed in rodent models of T2D [27]; acceleration of AD pathology in transgenic AD mice fed high fat and/or high sucrose diets [28–31]; antidiabetic treatment in humans with AD, and murine models of the disease show some improvement in cognition and memory and afford a certain level of protection against inflammation, apoptosis and synaptic failure in the brain [32, 33]. Finally, studies have recapitulated dysfunction in glucose metabolism, IR/PI3K/Akt signalling and the induction of inflammation and regulation of Tau and and Aβ processing in the brain following icv injection of the diabetogenic toxin, Streptozotocin (STZ) [see 34, 35]. Despite the number of studies and different approaches, they have produced mixed results that may be inherently linked with variables such as the type of model used, the duration of the experiments, type of diet, etc. Therefore, it is difficult to have a clear idea of how these dysfunctions link T2D to AD.

The aim of our experiments is therefore dual fold. Firstly, it is to determine whether a T2D profile might exacerbate dysfunctional mechanisms in CA1 of the hippocampus induced by early increases in soluble amyloid associated with preclinical stages of AD. To this end, we focussed on proteins in and associated with IR/PI3K/Akt signalling that contribute to deregulation of functions such as apoptosis, autophagy, inflammation, glucose uptake and the promotion of amyloid and tau processing [20, 21, 36]. Secondly. in an attempt to more closely mimic human T2D, we modified an established model of T2D that normally couples subdiabetogenic doses of Streptozotocin (STZ) with a calibrated high diet [37, 38] by coupling STZ injections with a human junk food (HJF) diet. In addition, we conducted longitudinal studies to determine the evolution of dysfunction induced by different treatments. Finally, as a functional readout, we repeatedly tested spatial recognition memory and subsequently the potential beneficial effect of environment enrichment (EE) has been shown to have general positive effects on hippocampal dependent memory including spatial and recognition memory and some forms of neuronal plasticity and mitigates deficits in rodent models of pathology [39, 40].

Material and Methods

Animals

Male Sprague Dawley rats ($n = 100$), weighing approximately 300 g, were purchased from Charles River Laboratories, France. The animals were housed in standard cages (2 rats/cage) and maintained in a temperature and humidity controlled colony room with 12/12-h light dark cycle with fresh water ad libitum and normal laboratory pellets (A04, SAFE, France) until the start the feeding protocol. All efforts were made to minimise the animal numbers and suffering throughout the experimental procedure. Experiments were conducted according to the European Communities Council Directive of 24 November 1986 (86/609/EEC), EU Directive 2010/63/EU, and the French National Committee (87/848), and approval from the local ethics committee (n°59).

General Protocol and Experimental Groups

We conducted longitudinal studies over 9–10 months, where rats were first started on a feeding regime of human junk food (HJF) and then 7 weeks later, injected twice with subdiabetogenic doses of Streptozotocin (STZ), 1 week apart. At week 20, some of the rats were implanted with osmotic minipumps containing soluble Aβ42 and the experiment was continued for another 15 weeks. Throughout the experimental period, regular glucose tolerance tests (GTTs) and spatial recognition memory tests were conducted (see timeline, Fig. 1). In western blotting, we also used brains from naïve rats for comparison with the control group.

Feeding Protocol

After 2 weeks' of adaptation to laboratory conditions, rats were randomly divided into two basic feeding regimes; those maintained on the calibrated laboratory diet (LD) at the recommended dose to maintain normal health and growth; or human 'junk' food (HJF; see Online Resource 1) that was high in calories, sugar and fat. Moreover, these foods contained chemical components used as stabilisers, emulsifiers, colourants, etc. A wide range of food products was offered to rats at the start of the experiment to determine their food preference and from a pool of about 20 foodstuff; 8–10 were given per day in excess, such that on a weekly basis, all rats ate the same foods in about the same quantity. This feeding regime was continued throughout the experimental period and body weight was recorded on a weekly basis. Consumption of major nutritional components in HJF was assessed each day over a 6-week period in the middle of the experiment.

Streptozotocin (STZ) Injections

STZ (Sigma- Aldrich) was dissolved in citric acid (pH 6.0), prepared as required and protected from light. Rats were fasted the night prior to given 2 sub-diabetogenic doses (30 mg/kg i.p.) 1 week apart approximately 7 weeks after the start of the feeding regime.

Amyloid-Beta (Aβ) Preparation, Infusion and Surgical Procedures

The Aβ42 peptide was specifically synthesised to be maintained in a soluble form, as reported elsewhere [41] and stored as lyophilised aliquots (0.1 mg) at − 80° until required. Prior to use, the peptide was resuspended in HyPure Molecular biology double distilled sterile water (Thermo; France), sonicated, diluted to a nominal concentration of 100 μM in aCSF (pH = 7.4, Alzet protocol), and filtered through a membrane filter (100 nm pore size, PVDF sterile, Millex, Millipore) to remove the insoluble aggregates. The final concentration was made in aCSF to 50 μM; the exact value was determined by a standard BCA assay.

For the TEM experiments, 10 μl aliquots were placed on formvar carbon 400-mesh copper grids (Electron Microscopy Sciences, Washington, PA, USA) after 168 h of incubation at 37 °C. Grids were stained with 2% (*w*/*v*) uranyl acetate. Specimens were studied with a Philips CM 10 transmission electron microscope (FEI Company, Hillsboro, Oregon, USA) operating at 100 kV. Images were taken by a Megaview II Soft Imaging System at a magnification of × 46000 and analysed with an AnalySis® 3.2 software package (Soft Imaging System GmbH, Münster, German).

Approximately 20 weeks after the start of the feeding regime, half of the rats in each group underwent surgery to implant osmotic minipumps (Alzet, model 2004, USA) to infuse Aβ42 intraventricularly (icv) over 7 days (0.5 μl/h). Rats were deeply anaesthetised with Ketamine (1.5 ml/kg) and Domitor (0.5 ml/kg). They were placed in a stereotaxic frame, the skull exposed to allow a single hole to be drilled out to place a cannula in the lateral ventricle (Bregma 1.3 mm; midline 1.8 mm; depth 3.0 mm from the brain surface). The cannula was connected to osmotic minipump via flexible tubing and fixed to the scalp with dental cement. The pump was then inserted subcutaneously between the scapula and the scalp incision was closed with surgical staples and swabbed with topical antiseptic and rats had a 5-day course of antibiotics.

Glucose Tolerance Test (GTT)

At different time points during the experiment (see Fig. 1), glucose tolerance tests were conducted. After overnight fasting, blood from the tail vein (approximately 4 μl each time) was sampled prior to (0 min) and 15, 30, 60 and 120 min following a bolus injection of glucose (i.p, 2 g/kg body weight, Sigma- Aldrich,). Blood glucose levels (mg/dL) were analysed using a glucometre (HemoCueR, Sweden). Analyses were conducted on basal (0 min) glucose levels and the area under curve (AUC) in response to the glucose challenge in each rat using Analysis of Variance (ANOVA).

Blood Insulin Assay

At the end of the experiment after overnight fasting, whole blood was collected immediately following sacrifice. Plasma was separated by centrifugation (3500 rpm, 25 min, at 4 °C) and stored at − 20 °C until analysis. Plasma insulin was measured using a Rat/Mouse Insulin ELISA Kit (Cat # EZRMI-13K, Millipore, Germany) according to the manufacturer's protocol and analysed using spectrophotometry (Molecular Device, France) at an absorbance level of 450 nm. Sample insulin concentrations (ng/ml) were calculated based on standard insulin curves and ANOVA was used to analyse group differences.

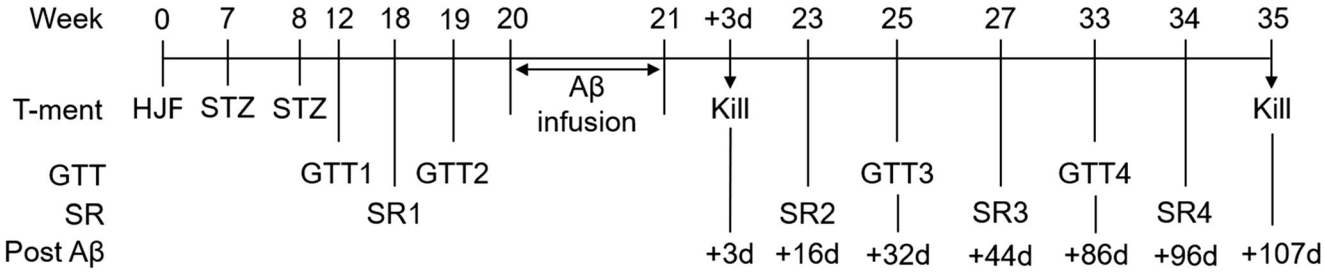

Fig. 1 Time line of experimental procedure. Protocol starts with HJF diet at week 0. Thereafter, different treatments across time the 35-week period are depicted. HJF, human junk food; STZ, streptozotocin; SR, spatial recognition memory tests; GTT, glucose tolerance tests; Aβ + indicates time following the end of infusion of Aβ

Recognition Memory Task

Recognition memory was conducted in a circular open field (diameter 90 cm, height 50 cm, painted black) in a room containing multiple 3-dimensional cues. Before training, rats were habituated to the open field (5 min/day, for 3 days). Following habituation, rats were given a sample phase (3 sessions of 4 min with a 4-min interval between sessions) where they explored three different objects constructed out of Lego™. At the first testing time point, we tested spatial recognition memory by changing the location of one of the objects during the sample phase following a 3 or 24 h delay, or object recognition memory by replacing one of the familiar objects for a novel one 24 h later. The test phase comprised a single session of exploration (4 min). Time spent exploring the objects was recorded via a video tracking system (ANYMAZE, Stoelting Co., USA). ANOVA was used to analyse the total time spent exploring objects during the sample phase to determine whether differences in exploration would indicate deficits in motor coordination or stress that may contribute to cognitive performance. Percent time spent exploring the novel location vs a mean of the two familiar locations was calculated to determine 50% as chance level using the Wilcoxon test and comparison between specific groups using Student's *t* test.

Environmental Enrichment

In a separate group of rats, we tested whether a mild form of environmental enrichment (EE), developed in the laboratory [42], would affect memory performance and protein regulation in a subset of rats in the STZ-HJF and control groups infused with Aβ or not. Groups of 4–5 rats were placed in a large wooden box (length 100 cm, width 80 cm, height 60 cm) containing junk objects for 3 h a day over 14 days. Objects were changed and repositioned every day. Rats were tested on the spatial recognition memory task after infusion of Aβ but prior to EE, and then several times after EE. In these experiments, we also tested memory with a 72-h delay after the sample phase.

Brain Tissue Preparation for Biochemical Analyses and Western Blotting Protocol

Rats were sacrificed by decapitation and CA1 of the hippocampus was dissected for analyses of expression and phosphorylation of proteins using immunowestern-blotting. Dissected tissue was immediately frozen in liquid nitrogen and kept at − 80 °C for later use. Proteins were extracted from the frozen tissue in lysis buffer [43]; and Complete Protease Inhibitor Cocktail and PhosSTOP (Roche, France). Homogenised samples were incubated on ice for 30 min and centrifuged at 15,000 rpm for 15 min at 4 °C; the supernatant was recovered and stored at − 80 °C. Protein concentrations were calculated using Bio-Rad protein assay (Bio-Rad, Germany) and samples were diluted with lysis buffer to give equal protein concentration of 1 μg/μl.

We used a standard western blotting protocol where 20 μl of samples was denatured in 5 x Laemmli sample buffer and boiled at 95 °C for 5 min before loading onto gradient acrylamide gels (6–12%). Proteins were separated using constant voltage (150 V) between 1.5 and 3 h and then transferred onto a nitrocellulose membrane (Amersham, GE Healthcare, Germany) by electro-blotting at a constant voltage (100 V; 90 min). Membranes were blocked with 5% non-fat dry milk (Bio-Rad, France) in TBS-T (Euromedex, France) and incubated overnight in primary antibodies at 4 °C with gentle shaking (see primary antibodies and dilution in Online Resource 2). Membranes were washed 3 times (5 min) in TBS-T and incubated in a horseradish peroxidase-conjugated anti-mouse/ rabbit immunoglobulin IgG secondary antibody (dilution 1:2000–1:10,000 in 5% BSA, Amersham, GE Healthcare, France) for 1–1.5 h at room temperature. Membranes were rinsed × 3 (5 min) in TBS-T and proteins were reacted with Chemiluminescence ECL solution (Amersham, GE healthcare, France), exposed to film (optimal exposure time for each antibody was maintained) and developed by hand. Membranes were subsequently washed and stripped (Re-blot plus; Millipore, Germany) and re-

incubated with other antibodies using the same procedure as described above. Protein bands were quantified using Gene Tools software (SynGene, Cambridge, UK). Total proteins were normalised to β-Actin and phosphorylated proteins to corresponding total protein. These were then normalised to the controls per gel as percent change. The relative changes in expression and phosphorylation of proteins were analysed statistically with Student's *t* test determined whether changes were significantly different from controls, and *t* test and/or ANOVA to determine group differences. The control group comprised a pool of naïve controls and those killed at either week 21 or 34 as preliminary analyses showed there were no significant differences between these groups.

Brain Tissue Preparation for Immunohistochemical Analyses of Aβ

Rats were deeply anaesthetised with pentobarbital (200 mg/kg, i.p.) and perfused transcardially with a solution containing 4% paraformaldehyde in 0.1 m phosphate buffer and brains were postfixed overnight in the same perfusion solution at 4 °C, immersed for 6 d in phosphate buffer containing 30% sucrose, and frozen in chilled 2-methylbutane (− 30 °C). Free-floating serial sections were pretreated with hydrogen peroxide to neutralise endogenous peroxidase activity. Non-specific binding sites were blocked with 4% normal goat serum. Sections were then incubated with the OC anti-Aβ polyclonal antibody (Euromedex, 1:3000) at 4 °C overnight. OC antibody recognises amyloid fibrillary deposits but also a subset of Aβ oligomers [44]. Incubation using secondary biotinylated goat anti-rabbit antibody (Vectorlabs) was then performed at room temperature for 2 h. The secondary antibody was finally detected by the peroxidase-avidin-biotin technique (ABC Elite Kit, Vector labs) with 3,3′-diaminobenzidine (DAB, Sigma-Aldrich) as chromogen. Sections were then collected on Superfrost glass slides, air-dried and finally dehydrated and cleared in grading alcohols and xylene and mounted in Eurokitt mounting medium. Sections were scanned with a NanoZoomer 2.0-RS slide scanner (Hamamatsu Photonics, pixel size 0.25 μm^2) to generate virtual slides. Following Aβ immunohistochemistry and scanner digitization, 3 regions of interest (dorsal hippocampus, prefrontal cortex, corpus callosum) were manually outlined on microphotographs (3 sections/region/rat). The optical density (OD) of each brain area was assessed using the MCID Elite image analysis software (Linton, Cambridge, UK). OD was normalised relative to the staining of the corpus callosum, which served as baseline value to obtain relative optical densities (ROD) of the prefrontal and hippocampal regions. Statistical analyses were conducted using the non-parametric Kruskall-Wallis and Mann Whitney tests.

Results

We conducted experiments over 35 weeks to determine whether coupling STZ injections with HJF would induce classic T2D characteristics and whether infusion of Aβ42 would exacerbate a functional readout (hippocampal-dependent memory) and basal regulation of protein in and associated with IR/PI3K/Akt signalling in CA1 of the hippocampus (see timeline of treatments depicted in Fig. 1).

T2D Characteristics: Food Intake and Weight Gain

As the aim of our experiment was to mimic human food consumption rather than an extensive study on the effect of different nutritional categories of food stuffs, we made cursory analyses of the food consumption over a 6-week period in the middle of the experiment in a subgroup of rats fed laboratory diet (control and STZ; $n = 13$) and cafeteria diet (HJF and STZ-HJF; $n = 11$). Rats fed HJF, consumed nearly twice the amount of calories per week (853 kcal) compared with those fed Laboratory Diet (LD, 488 kcal; $p < 0.01$ Wilcoxon test; Fig. 2a). In terms of the major nutritional food groups, rats fed HJF consumed about the same amount of carbohydrates as those fed LD ($p > 0.05$; Wilcoxon test); less overall protein content ($p < 0.01$; Wilcoxon test) but more lipids ($p < 0.01$; Wilcoxon test, Fig. 2b). However, the amount of sugar contained in the HJF was approximately 49.4% whereas in LD it was 3.7%, and protein content in HJF was mainly derived from animal proteins whereas it was at least 66% vegetable proteins in LD. The other major differences in nutritional composition are shown in Fig. 2d.

Weight was measured on a weekly basis; at the start of experiment, all rats had the same weight ($F < 1$), but across time, those fed HJF (HJF and STZ-HJF) gained significantly more weight than those groups fed LD (controls and STZ). By the end of the experiment, rats fed HJF gained approximately 25% more weight than those on the control diet ($F(3,96) = 12.78$; $p < 0.0001$; see Fig. 2c).

T2D Characteristics: Plasma Glucose Levels

We conducted 4 glucose tolerance tests (GTT) at different time points throughout the experimental period (see timeline; Fig. 3a) and used ANOVA and Tukey post hoc analyses. Basal glucose levels in the first (week 12: $F(3,82) = 2.79$; $p < 0.05$) and second test (week 19: ($F(2,57) = 5.34$; $P < 0.01$) were modestly but significantly increased only with STZ-HJF treatment compared with controls. By the third (week 25: $F(3,31) = 9.71$; $p < 0.001$) and fourth (week 33: $F(3,31) =$

8.84; $p < 0.001$) tests, basal glucose was greatly elevated in STZ-HJF treated rats compared with controls but also with STZ and HJF treatment (all post hoc values $p < 0.05$; Fig. 3b).

At the same time points, we also assessed plasma glucose levels following a glucose challenge using a standard glucose tolerance test (GTT) and analysed the area under the curve (AUC). In all 4 tests, STZ-HJF treated rats showed a significantly greater AUC value compared with all other groups (week 12: $F(3,81) = 21.63$; $p < 0.001$; week 19: $F(2,57) = 12.17$; $p < 0.001$; week 25: $F(3,29) = 7.33$; $p < 0.001$; week 33: $F(3,32) = 12.42$; $p < 0.001$; all post hoc analyses; $p < 0.05$; Fig. 3c).

Repeated measures ANOVA and post hoc analyses on the subgroup of STZ-HJF treated rats tested at all time points showed a significant difference in basal glucose levels ($F(3,18) = 1.43$; $p < 0.01$) and AUC ($F(3,18) = 6.48$; $p < 0.01$) between the first 2 and the last two tests (post hoc analyses, $p < 0.05$; Fig 3b, c) and this is reflected in Fig. 3d, e showing glucose curves per group in mg/dL in the first and last test. In summary, only STZ-HJF treated rats showed obvious hyperglycemia as they had a consistent increase in basal fasting plasma glucose and impaired glucose tolerance in response to glucose challenge that evolved with time. Moreover, repeated measures ANOVA and post hoc analyses on the subgroup of STZ-HJF treated rats tested at all time points ($F(3, 18) = 1.43$; $p < 0.01$) showed a significant difference in glucose levels between the first 2 tests and the last two tests (post hoc, $p < 0.05$).

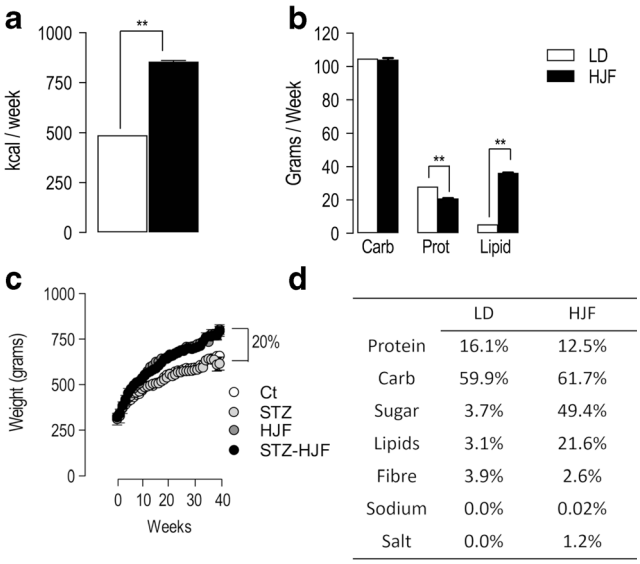

	LD	HJF
Protein	16.1%	12.5%
Carb	59.9%	61.7%
Sugar	3.7%	49.4%
Lipids	3.1%	21.6%
Fibre	3.9%	2.6%
Sodium	0.0%	0.02%
Salt	0.0%	1.2%

Fig. 2 Food intake and weight gain. **a** Shows the relative caloric intake in rats fed LD ($n = 13$) or HJF ($n = 11$). **b** Indicates the consumption of major food groups, Carb, Prot, and Lipids. **c** Weight gain in the 4 major groups Ct and STZ alone (both fed LD), HJF alone and STZ-HJF (both fed HJF). **d** Percentage of nutritional components in LD and HJF. STZ, Strepotozotocin, HJF, human junk food diet; LD, laboratory diet; Carb, carbohydrates; Prot, protein. ** $p < 0.01$

T2D Characteristics: Basal Plasma Insulin Levels

At the end of the experiment, plasma insulin was measured using ELISA. ANOVA showed very high levels in rats fed HJF ($n = 8$) that is a common feature of obesity [19]; with a slight but non-significant increase in rats in the STZ group ($n = 5$) compared with controls ($n = 7$). In STZ- HJF treated rats insulin levels at week 21 ($n = 5$) were hugely increased above control levels and even that observed in rats in the HJF group. However, by the end of the experiment (week 35; $n = 4$), this early increase was dramatically decreased, such that there was no longer any difference between this group and controls ($F(4,19) = 32.83$; $p < 0.001$; Fig. 4a).

To compare the relationship between glucose and insulin, we normalised plasma insulin and glucose levels, in the last test to their corresponding controls (Fig. 4b). In rats in the HJF group, there was a huge and significant increase in insulin levels compared with relatively normal levels of glucose ($t = 7.89$; $p < 0.001$) suggesting either insulin resistance and/or hyperinsulinemia. At week 21, STZ-HJF treated rats showed a similar relationship between glucose and insulin as that

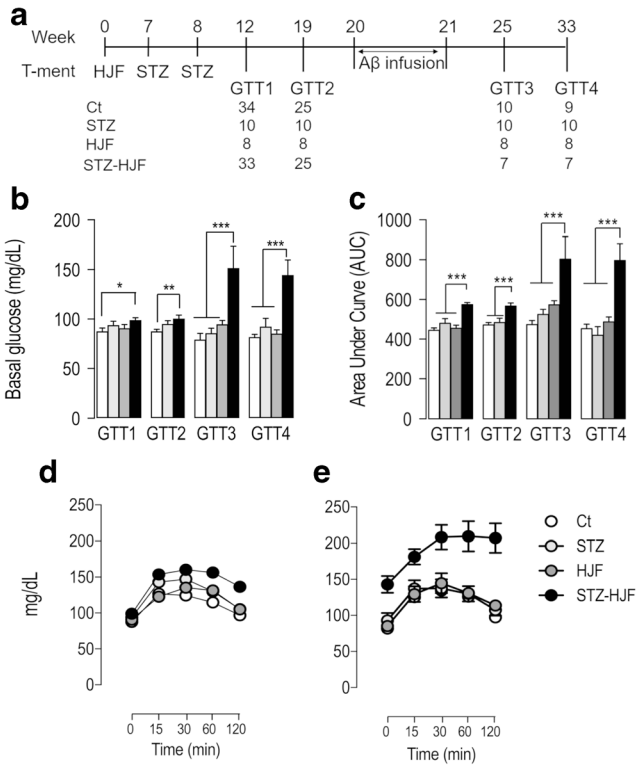

Fig. 3 Plasma glucose regulation. **a** Depicts the time line and numbers of animals tested in each group. **b** Shows evolution of fasted basal glucose levels (0-time point; mg/dL) across the 4 time points. **c** Shows area under curve (AUC) of individual response curves to a glucose challenge. Statistical analyses were conducted on AUC, figures **d** and **e** show the mean group differences of the response curves in first test (**d**) and the last test (**e**) in mg/dL. Data is represented as mean ± SEM; *$p > 0.05$; **$p < 0.01$; ***$p < 0.001$. NB the HJF group alone was not test at GTT2

observed with HJF, inasmuch as there was relatively no change in glucose levels and substantially high levels of insulin (t = 18.73; $p < 0.001$). In contrast, by week 35, STZ- HJF treated rats showed an increase in glucose with a relative decrease in insulin compared with glucose levels (t = 2.36; $p < 0.05$) and with insulin levels at the earlier time point (t = 5.35; $p < 0.01$), with no difference in the ratio of glucose to insulin (t = 0.69; $p > 0.05$). As only the STZ-HJF treatment induced the classic signs of a T2D phenotype, we subsequently focussed on this group for behavioural experiments. Rats injected with STZ alone or were fed HJF diet alone did not undergo memory tested or were subjected to environmental enrichment.

Memory Deficits Induced by STZ-HJF Treatment

To test whether the STZ-HJF treatment impacted memory, we tested recognition memory 4 times throughout the experimental period (see time line; Fig. 5a). In the first test at approximately week 18, we tested rats using spatial recognition memory, where the location of one object was changed following a 3-(SR3h) or 24-(SR24h) hour delay, and object recognition, where one object was replaced with a novel one following a 24-(OR24h) hour delay. We found rats treated with STZ-HJF showed no deficit compared with control in spatial recognition with a 3-h delay (t = 1.72; $p < 0.05$). However, with a 24-h delay, there was a modest but significant deficit compared with controls (t = 7.3; $p < 0.0001$); albeit their performance was significantly greater than chance level (Wilcoxon test: $p < 0.0001$ compared with 50%). In addition, there was no deficit in novel object recognition (OR) at 24 h (t = 1.83; $p < 0.05$, Fig. 5b); therefore, we continued only with spatial recognition with a 24-h delay. Here, we found the same modest deficit in the subsequent tests compared with controls (week 23; t = 6.82; $p < 0.0001$; week 27: t = 6.73; $p < 0.0001$; week 34: t = 6.3 $p < 0.0001$) but performance was still significantly above chance (all $p < 0.001$, Wilcoxon test). In all 4 SR24h tests, during the sample phase, rats showed equal exploration of the 3 objects compared with the control group (all tests, $p > 0.05$; data not shown), suggesting the STZ-HJF treatment had no discernible effect on locomotor activity, stress or the normal tendency for exploring objects. Together, this suggests that STZ-HJF treatment impaired spatial recognition memory, but this was a modest deficit. Moreover, the impairment remained remarkably stable across time (Fig. 5c).

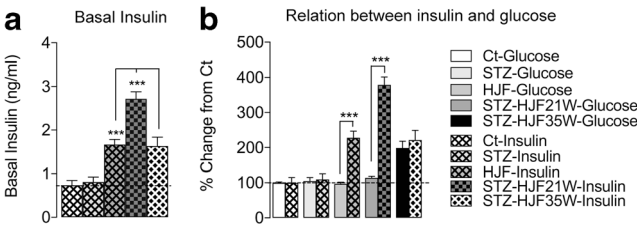

Fig. 4 Plasma insulin regulation. **a** Plasma insulin levels (ng/ml) at the end of the experiment in the 4 experimental groups. **b** Relationship between glucose (solid bars) at the last test and insulin (hatched bars) when killed. Data are normalised to respective control levels and are represented as % change. NB, STZ-HJF group is measured at two time points. Data are represented as mean ± SEM; ***$p < 0.001$. Ct ($n = 7$); HJF ($n = 8$); STZ $n = 5$); STZ-HJF-21 W ($n = 5$); STZ-HJF-35 W ($n = 4$)

Infusion of Aβ Alone, and in Conjunction with STZ-HJF Treatment on Spatial Recognition Memory

We tested rats on spatial recognition memory with a 24-h delay prior to infusion of Aβ to establish a baseline level of performance, and at 3 time points after (see time line Fig. 6a). Quite simply, control rats infused with Aβ showed a deficit 16 days following infusion compared with non-infused counterparts (t = 10.92; $p < 0.001$), but recovered to control levels by day 44 post infusion (t = 1.68; $p > 0.05$) and this was maintained at 96 days post infusion (t = 1.03; $p > 0.05$; Fig. 6b).

As expected, 16 days following infusion of Aβ rats with STZ-HJF treatment showed a deficit in performance as it dropped to chance level, compared with non-infused STZ-HJF treated rats (t = 4.57; $p < 0.0001$) and this deficit was maintained for the next two tests (44 and 96 days post-Aβ infusion) compared with non-infused STZ-HJF treated rats (day 44: t = 5.97; $p < 0.001$; day 96: STZ-HJF: t = 5.05; $p < 0.001$; Fig. 6c). These data suggest infusion of soluble Aβ42 alone induced a temporary deficit in performance in a spatial recognition task; however, on a T2D background, the deficit is prolonged.

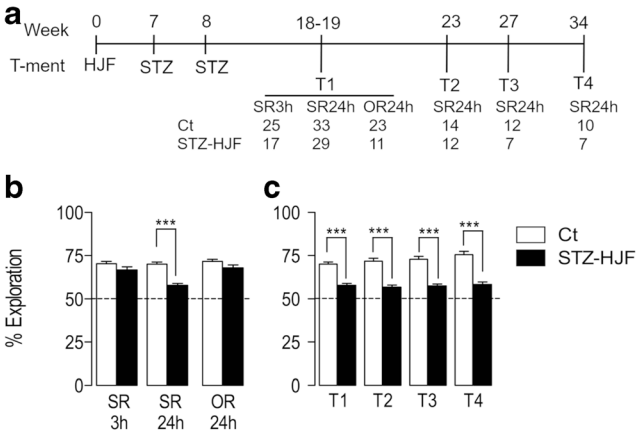

Fig. 5 Effect of STZ-HJF treatment on different forms of recognition memory. **a** Depicts the time line of memory testing and numbers of animals at each test. **b** Shows the per cent exploration of the novel location at 2 different time intervals and percentage exploration of a novel object with a 24-h delay. **b** Shows % exploration of the novel location with a 24-h delay at different time points throughout the experiment. Data is represented as mean ± SEM; ***$p < 0.001$. SR3h, spatial recognition memory with a 3-h delay; SR24h, spatial recognition memory with a 24-h delay; OR24h, object recognition memory with a 24-h delay

Beneficial Effect of Environmental Enrichment on Recognition Memory Performance

We first tested whether EE had a beneficial effect on memory performance, using 2 delays between sample and test phases (24 and 72 h) at different time points following EE. We found enriched rats showed no beneficial effect compared with home-caged rats when the retention delay was 24 h (31 days post EE: $t = 0.75$; $p > 0.05$; 60 days post EE: $t = 0.38$, $p > 0.05$). When the delay was extended to 72 h, enriched rats maintained the same level of performance as they did with a 24-h delay; however, in home-caged rats, although their performance was significantly greater than chance level (Wilcoxon test, $p < 0.01$ at both time points), it was significantly poorer compared with enriched rats ($t = 2.64$; $p < 0.05$ and $t = 2.68$; $p < 0.05$ at both time points). These data suggest with a 24-h delay, all rats had reached asymptotic level of performance; however, when increasing the demand on memory by increasing the retention delay, EE endowed a long lasting beneficial effect (Fig. 7a).

We used the same protocol to test whether EE could benefit rats infused with Aβ alone and those receiving STZ-HJF and STZ-HJF + Aβ treatment (time line, Fig. 7b). The first test (24-h delay) was after Aβ infusion but prior to EE and served as a baseline effect for EE. Aβ infusion in both controls ($t = 6.71$; $p < 0.001$) and STZ-HJF treatment ($t = 3.2$; $p < 0.05$) induced poorer performance when compared with that of their non-infused counterparts as we have shown in the previous experiment (Fig. 7c, d). The first two tests post EE were conducted with a 24-h delay and control rats infused with Aβ showed equivalent performance compared with non-infused controls (EE+4 days: $t = 1.56$; $p > 0.05$; EE+39 days: $t = 0.97$; $p > 0.05$; Fig. 7c). EE+4 days is within the time window in which Aβ impairs performance, but EE+39 days is out with the time window, confirming the recovery is stable (Fig. 6b). However, when a 72-h delay was imposed in tests outside the Aβ time window; performance in Aβ-infused rats dropped 17 days post EE, although did not reach statistical significance compared with controls ($t = 2.18$; $p = 0.07$). Performance, however, recovered to control levels ($t = 1.56$; $p > 0.05$) by the last test (EE+47 days, Fig. 7c). Together, the data suggests when the retention interval is increased, imposing a greater demand on memory, the deleterious effect of Aβ is still observed at 17 days post EE, but has recovered by EE+47.

With the first test following EE (EE+4 days), both STZ-HJF treated rats ($t = 9.56.0$; $p < 0.001$; paired t test) and those infused with Aβ ($t = 2.8$; $p < 0.05$) showed improved performance compared with that prior to EE; however, despite the improvement, STZ-HJF-treated rats infused with Aβ had significantly poorer performance than non-infused counter parts ($t = 4.21$; $p < 0.01$). By the second test (EE+39 days), the beneficial effect observed 4 days post EE in both groups had dropped back to pre-EE levels with no significant difference

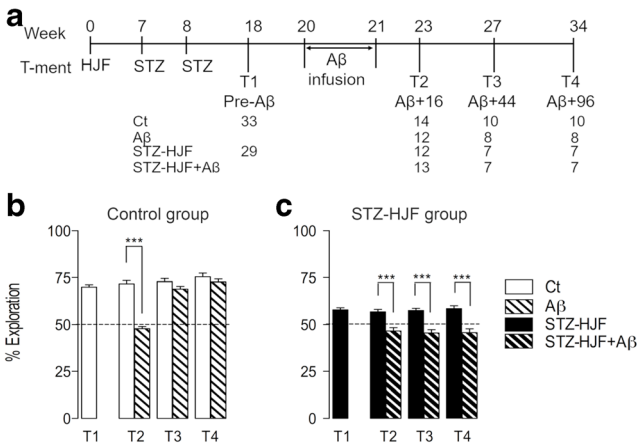

Fig. 6 Effect of Aβ alone/in conjunction with STZ-HJF treatment on spatial recognition memory with a 24-h delay. **a** Shows the time line of testing and the number of animals per group. **b** Histograms represent percent exploration of the novel location at different time points in controls and rats infused with Aβ alone. **c** Histograms represent % exploration of the novel location at different time points in STZ-HJF and STZ-HJF + Aβ treated rats. NB, non-infused groups are the same as those depicted in Fig. 5. Data is represented as mean ± SEM; ***$p < 0.001$

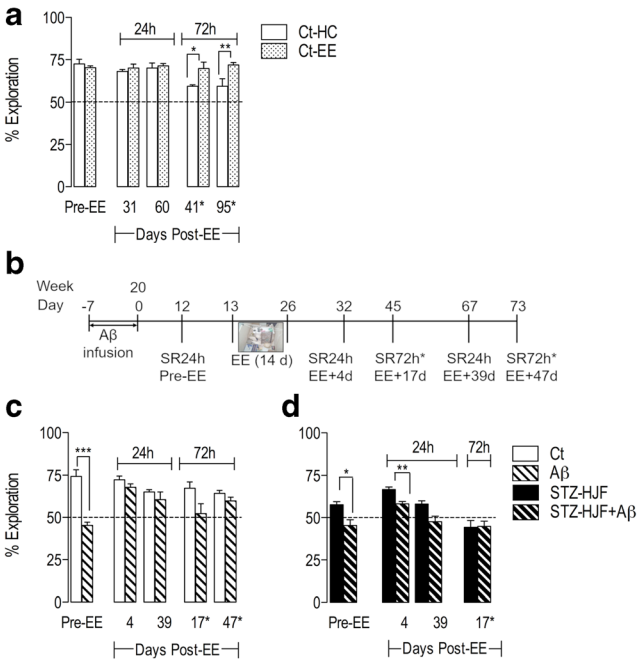

Fig. 7 The effect of environmental enrichment (EE) on control and STZ-HJF treated rats infused with Aβ. **a** An initial experiment determined the impact of EE ($n = 5$) in control rats compared with home-caged ($n = 5$) at different times following EE. Time-delay between the sample and test phase is either 24 or 72 h. **b** Represents the time line of experimental testing for the effect of EE on STZ-HJF treated and control rats. **c** Memory capacity in control rat infused with Aβ or not; prior to and at different time points after EE. **d** Represent STZ-HJF treated rats infused with Aβ or not at the same time points as control rats. Data is represented as mean ± SEM; *$p < 0.05$; **$p < 0.01$; ***$p < 0.001$. Ct ($n = 4$); Aβ ($n = 5$); STZ-HJF ($n = 4$); STZ-HJF+ Aβ ($n = 5$)

between the 2 time points (STZ-HJF: t = 0.15; $p > 0.05$; STZ-HJF + Aβ: t = 2.48; $p < 0.05$; paired *t* tests). With the first test with a 72-h delay (EE+17 days), both groups were at chance level (STZ-HJF: $p > 0.05$; STZ-HJF + Aβ: $p > 0.05$; Wilcoxon test), suggesting the beneficial effect of EE was short lasting; therefore, these rats underwent no further testing (Fig. 7d).

Protein Regulation by STZ-HJF Treatment Coupled with Infusion of Aβ

We found the combined STZ-HJF + Aβ treatment regulated all protein expression and phosphorylation with the exception of expression of Akt and NFκB compared with controls at either week 21 (3 days post infusion of Aβ) or week 35 (17 weeks post infusion of Aβ), and, although phosphorylation of BAD was increased at 21 weeks, it was not sustained (Table 1, columns F, G). In terms of the evolution of changes, we found 4 different patterns of regulation. (1) Those proteins regulated at 21 weeks and maintained, and in general, these constituted an increase mainly in expression of mTOR, BAD, FoxO3 and phosphorylation of mTOR (see *p* values indicated by asterisks in Table 1); albeit pmTOR had significantly reduced phosphorylation by week 35 compared with week 21 (t = 3.83; $p < 0.01$). However, comparison of phosphorylation of mTOR against expression of mTOR respective proteins at either time point was no different from that of controls ($F(1,3) = 0.24$; $p > 0.05$; Table 1). (2) A second pattern was a change in levels at 21 weeks that was exacerbated by 35 weeks that included a decrease in expression of GluT-1 (t = 5.87; $p < 0.01$). (3) Thirdly, there was a change in one direction at 21 weeks that was reversed above control levels including an early decrease that reversed to increased expression of Gsk3β (t = 4.49; $p < 0.01$) and phosphorylation of NFκB (t = 6.42; $p < 0.001$) and conversely, the increase in pGsk3β reversed to a decrease (t = 4.21; $p < 0.01$). (4) Finally, there was a late developing increase in the expression of APP, and decrease in expression of IDE, Beclin-1 and pAkt in the absence of change at week 21 (Table 1).

Protein Regulation by STZ-HJF Treatment Alone

Only a subset of proteins were regulated by STZ-HJF treatment alone compared with those regulated by the group infused with Aβ (Table 1, columns B, C); and in general, most of these proteins were regulated in the similar manner to the STZ-HJF + Aβ group. These included an increase in expression of BAD and FoxO3 at week 21 that was maintained up to 35 weeks. Similarly, regulation of pNFκB went from an early decrease to a late increase (t = 8.17; $p < 0.001$; Fig. 8a,c). The only difference was in regulated expression of mTOR, which although was increased at week 35, as with the STZ-HJF + Aβ group, it was not increased at the early time point (Table 1). Importantly, STZ treatment alone had negligible effects on protein regulation; it induced an increase in expression of mTOR that was significantly elevated compared with control rats (t = 3.05; $p < 0.01$) and, although less than that induced by the combined treatment, it was not a significant difference (t = 0.92; $p > 0.05$). HJF alone also induced a similar increase in mTOR (t = 2.75; $p < 0.05$) FoxO3 (t = 4.18; $p < 0.001$) that was equivalent to the levels induced by STZ-HJF and STZ-HJF + Aβ treatments (*p* values > 0.05). This suggests, in particular, HJF might be responsible for the changes in some of these proteins induced by STZ-HJF treatment (Online Resource 3).

Protein Regulation by Aβ Alone

As with STZ-HJF treatment, Aβ alone induced only a subset of changes in protein levels compared with STZ-HJF treated rats infused with Aβ. Of the proteins regulated by Aβ, the majority of them showed early regulation at 21 weeks (3 days post Aβ infusion) but were not sustained that would argue for the peptide being eliminated. These include an early decrease in expression of Gsk3β and GluT-1 and an increase in expression of BAD. This is in keeping with the early deficit in memory performance that recovers with time. Expression of FoxO3 was increased at 21 weeks and maintained, but similarly to STZ-HJF treatment. Finally, in a similar manner to STZ-HJF treatment, there was a delay in the increase in expression of mTOR at week 35 (Table 1 columns D, E).

This synthetic form of Aβ42 induces small round oligomers with diameters of 3 to 30 nm analysed by transmission electron microscopy (TEM; Fig. 9a) and remains relatively stable for a long time [41]. We also found no evidence of fibrillar or classic aggregated Aβ in the dorsal hippocampus at the end of infusion of the peptide compared with control rats (U = 4; $p > 0.05$, Mann Whitney) or between control ($n = 4$) and STZ-HJF treated rats ($n = 3$; H = 4.79; $p > 0.05$, Kruskall-Wallis) at the end of the experiment (Fig. 9b). At week 35, OC immunostaining showed weak but significant diffuse staining in all groups (Fig. 9c) that was absent from control negative sections (primary antibody omission, data not shown) that contrasted sharply with control positive sections (tissue from an old APPxPS1 transgenic mouse harbouring severe brain amyloidosis, data not shown). OC immuno staining therefore suggests that Aβ was in a prefibrillar form [44]. Although we did not biochemically analyse Aβ42 and therefore cannot whether infusion of the peptide was still present in the brain by the end of the experiment, the data suggest that at least it was non longer at an effective level to induce a deficit in memory and dysregulation of many proteins.

Table 1 Values of group means of optical density presented as a % change from control rats

A	B STZ-HJF-W21 $n = 5$	C STZ-HJF-W35 $n = 4$	D Aβ W21 3 days post Aβ $n = 6$	E Aβ W35 17 weeks post Aβ $n = 5$	F STZ-HJFAβ W21 3 days post Aβ $n = 5$	G STZ-HJFAβ W35 17 weeks post Aβ $n = 5$	H Ct-EE-W35 17 weeks post Aβ 9–10 weeks post EE $n = 4$	I Aβ-EE-W35 17 weeks post Aβ 9–10 weeks post EE $n = 4$	J STZ-HJFEE-W35 17 weeks post Aβ 9–10 weeks post EE $n = 5$	K STZ-HJF-Aβ-EE-W35 17 weeks post Aβ 9–10 weeks post EE $n = 5$
Akt	104.8± 2.9	100.5± 2.5	97.7± 2.8	105.9± 2.0	100.7± 5.4	108.9± 4.6	103.0± 3.8	94.2± 3.9	104.4± 4.5	99.5± 4.5
pAkt	105.8± 7.3	102.8± 4.2	95.4± 7.1	98.0± 2.8	100.2± 5.5	⇓77.6± 4.7**#	99.2± 7.4	102.7± 3.3	109.0± 4.4	104.2± 5.9§
mTOR	100.1± 7.6	⇑141.4± 3.5**#	98.7± 12.0	⇑143.4± 9.0***#	⇑148.7± 6.4***	⇑159.2± 9.3***	103.4± 0.8	⇑144.2± 7.4***§	⇑133.9± 3.7**	⇑172.2± 10.8***
pmTOR	92.23± 7.1	102.1± 3.5	91.2± 7.1	97.0± 4.1	⇑165.9± 24.2***	⇑126.9± 4.8**#	101.3± 4.7	104.0± 8.3	91.8± 2.3	95.3± 2.0§
Beclin-1	106.9± 5.2	98.8± 2.1	106.5± 4.4	94.3± 6.2	109.1± 8.4	⇓75.6± 1.9***#	90.7± 2.4	91.0± 6.4	90.7± 6.0	⇓75.5± 9.8**
Gsk3β	100.4± 4.2	94.8± 5.9	⇓82.2± 3.9***	97.6± 2.6	⇓77.3± 4.8***	⇑124.0± 2.7***#	99.7± 2.5	97.2± 4.9	93.9± 5.9	⇑127.1± 4.9**
pGsk3β	108.3± 2.2	102.0± 2.4	95.7± 8.0	104.3± 3.9	⇑149.5± 15.3***	⇓82.3± 4.5**#	106.4± 8.1	110.1± 8.1	107.4± 6.8	⇑120.7± 5.9***§
BAD	⇑129.8± 4.3***	⇑131.8± 2.4***	⇑148.0± 10.2***	93.7± 6.4#	⇑145.0± 5.8***	⇑150.9± 2.2***	103.4± 2.2	101.2± 6.0§	105.9± 2.2§	⇑117.2± 3.3***§
pBAD	101.4± 2.4	95.8± 3.4	93.4± 9.1	106.7± 4.7	⇑135.0± 4.3***	100.1± 3.4#	107.2± 4.4	99.3± 6.3	96.0± 3.6	99.0± 2.0
FoxO3	⇑128.7± 8.0*	⇑140.5± 3.5**	⇑131.9± 8.4*	⇑132.2± 5.2**	⇑132.6± 16.4*	⇑133.8± 6.5**	100.2± 9.3	⇑136.1± 15.2*	⇑144.0± 8.8**	⇓136.4± 8.5**
IDE	99.1± 2.2	99.8± 2.8	106.0± 4.2	102.8± 6.5	98.3± 6.7	⇓72.2± 4.17***#	104.0± 2.5	106.2± 1.7	⇑141.9± 5.7***§	98.9± 3.8§
APP	95.5± 6.2	93.6± 4.8	96.4± 3.6	90.9± 3.6	109.6± 0.9	⇑135.5± 2.4***#	95.5± 2.2	99.0± 1.2	102.9± 0.7	⇑122.6± 8.**
NF|B	108.5± 8.2	99.7± 4.5	102.8± 3.8	94.6± 7.7	106.5± 3.9	90.2± 5.3	106.4.7± 16.1	95.3± 8.9	89.9± 17.0	93.5± 12.9
pNF|B	⇓64.9± 4.5**	⇑139.1± 7.3**#	97.6± 3.3	94.9± 9.2	⇓72.5± 8.4*	⇑132.5± 4.1**#	106.6± 16.1	100.7± 18.4	88.8± 12.6§	86.6± 9.5§
Glu-T1	115.7± 4.3	105.5± 5.9	⇓67.9± 7.3***	93.2± 7.9#	⇓72.0± 5.3***	⇑36.5± 2.8***#	⇑195.3± 21.1***§	⇑162.7± 9.0***§	⇑237.4± 24.5***§	⇑217.1± 29.0***§

*Indicated where there values are significantly changed from controls using Student's *t* test. ***$p < 0.001$, **$p < 0.01$, *$p < 0.05$. Arrows indicate the direction of change. #Indicates where proteins levels measured at 35 weeks (17 weeks post Aβ infusion) are significantly change from the earlier time point of 21 week (3 days post Aβ infusion). §Applies to EE only and indicates where EE induces a significant change compared with non EE counterparts

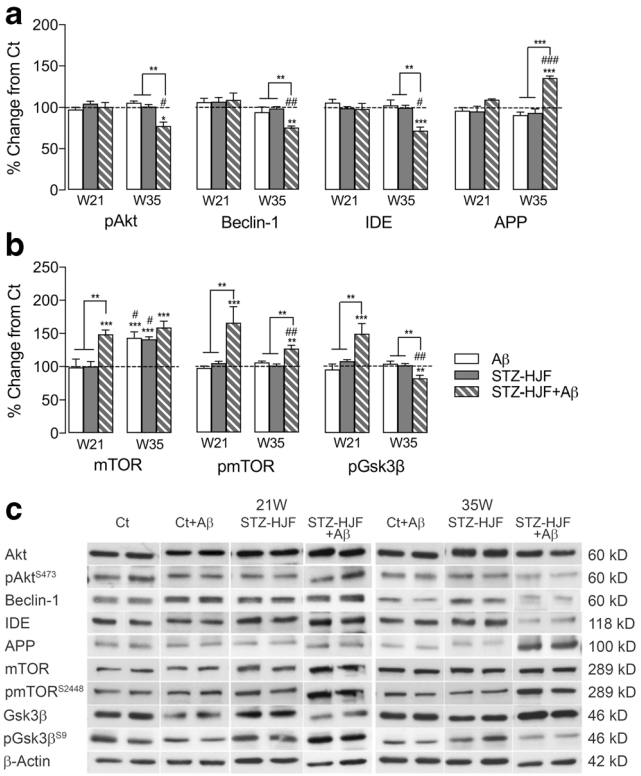

Fig. 8 Regulation of proteins specific to STZ-HJF + Aβ treatment. Group means±SEM are represented for Ct + Aβ ($n = 5$); STZ-HJF ($n = 5$); STZ-HJF + Aβ ($n = 4$) at W21 and Ct + Aβ ($n = 5$); STZ-HJF ($n = 5$); STZ-HJF + Aβ ($n = 5$). **a** Represents changes in basal proteins specific to STZ-HJF + Aβ treatment that develop by the late time point (35 weeks); **b** represents changes in basal proteins specific to STZ-HJF + Aβ treatment that evolve across time; **c** sample western blots represent the group mean of each protein, including the control group ($n = 16$). NB as statistical analyses was based on the % change from control; the representative band is the same in Figs. 11 and 12. Asterisks above histograms represent significant change from controls, and those above the bars represent significant differences between groups; *, $p < 0.05$; **, $p < 0.01$; ***, $p < 0.001$. # indicates difference between each group at the two different time points, #, $p < 0.05$; ##, $p < 0.01$; ###, $p < 0.001$

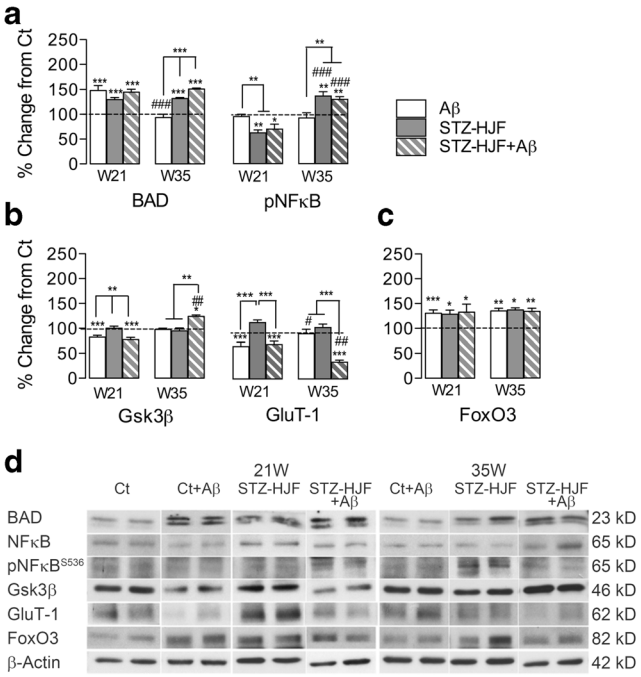

Fig. 9 Regulation of proteins induced by treatments independently. Group means±SEM are described in the legend of Fig. 8. **a** Protein regulation we attribute to STZ-HJF treatment alone. **b** Protein changes in which infusion of Aβ at least contributes to changes induced by STZ-HJF + Aβ. **c** Increase in Fox03 is regulated by all treatments independently. **d** Sample western blots represent the group mean of each protein, including the control group ($n = 16$). Asterisks indicate significant changes from control rats, *, $p < 0.05$; **, $p < 0.01$; ***, $p < 0.001$. # indicates differences between each group at the two different time points, #, $p < 0.05$; ##, $p < 0.01$; ###, $p < 0.001$

Impact of Environmental Enrichment on Expression and/or Phosphorylation of Proteins

Protein regulation was tested 9–10 weeks following the end of EE at week 35, as in all other experiments. We first asked what the impact EE alone was and found only Glu-T1 expression was increased in control enriched animals ($t = 8.32$; $p < 0.001$), but also in all other groups compared with non enriched counterparts (Table 1, column H, Fig. 10a); however, there was no significant difference between groups ($F(1,3) = 0.29$; $p > 0.05$). We then asked whether EE could reverse changes induced by STZ-HJF treatment coupled with infusion of Aβ. Specific to STZ-HJF + Aβ treated rats, EE rectified the decrease in pAkt ($t = 3.34$; $p < 0.05$) and the increase in pmTOR ($t = 6.56$; $p < 0.001$) to control levels and induced an increase in pGsk3β compared with controls ($t = 2.84$; $p < 0.01$) and non-enriched counterparts ($t = 4.93$; $p < 0.01$, Fig. 10b). However, as both increase in expression of mTOR and Gsk3β were not modified by EE (see Fig. 11), the relative change in phosphorylation of these proteins suggests Akt has a negligible effect. EE also modified phosphorylation of pNFκB and expression of IDE and BAD induced by STZ-HJF treatment whether infused with Aβ or not (Table 1, Fig. 10c). It reversed the increase in pNFκB induced by STZ-HJF alone ($t = 3.22$; $p < 0.05$) and STZ-HJF + Aβ ($t = 4.03$; $p < 0.01$) to control levels.

Although STZ-HJF treatment alone did not modify expression of IDE, EE induced a significant increase compared with controls ($t = 7.23$; $p < 0.001$) and non-enriched counterparts ($t = 6.05$; $p < 0.001$) and increased expression of IDE in STZ-HJF + Aβ treated rats compared with non-enriched counterparts ($t = 4.73$; $p < 0.01$) that only reach control levels (Table 1, columns G, K). Similarly, the increase in expression of BAD was significantly decreased in both groups compared with non-enriched counterparts (STZ-HJF: $t = 8.1$; $p < 0.001$; STZ-HJF + Aβ: $t = 8.06$; $p < 0.001$); however, the decrease in STZ-HJF + Aβ treated rats was still elevated compared with controls ($t = 4.46$; $p < 0.001$; Fig. 10c), suggesting that in both enriched and non-enriched rats, phosphorylation of BAD in both groups was still in an active state. Finally, STZ-HJF +

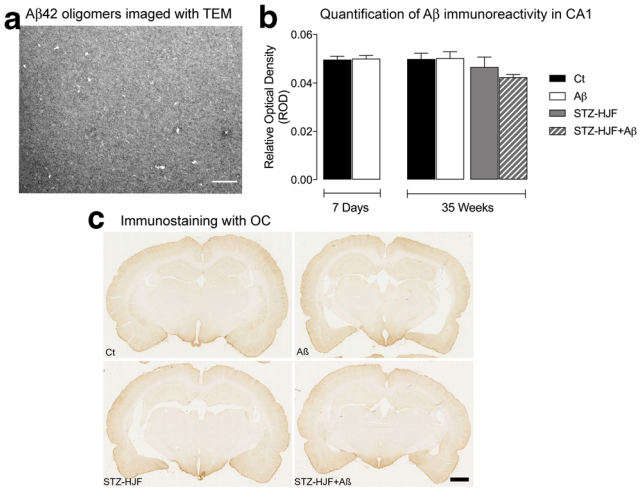

Fig. 10 Aβ42 peptide. **a** TEM image of Aβ oligomers following 1 week of incubation in aCSF at 37 °C. Small, round oligomers could be detected with diameter in the range of 3 to 30 nm. Scale bar 200 nm. **b** Relative optical density (mean ± SEM) of Aβ immunoreactivity in control ($n = 4$) and Aβ ($n = 3$) infused rats 7 days after infusion of Aβ and at 35 weeks post infusion in control ($n = 4$) Aβ-infused rats ($n = 3$), STZ-HJF treatment ($n = 3$) and STZ-HJF + Aβ treatment ($n = 3$). **c** Microphotographs of the dorsal hippocampus show diffuse staining after incubation with OC antibody. Scale bar 2 mm

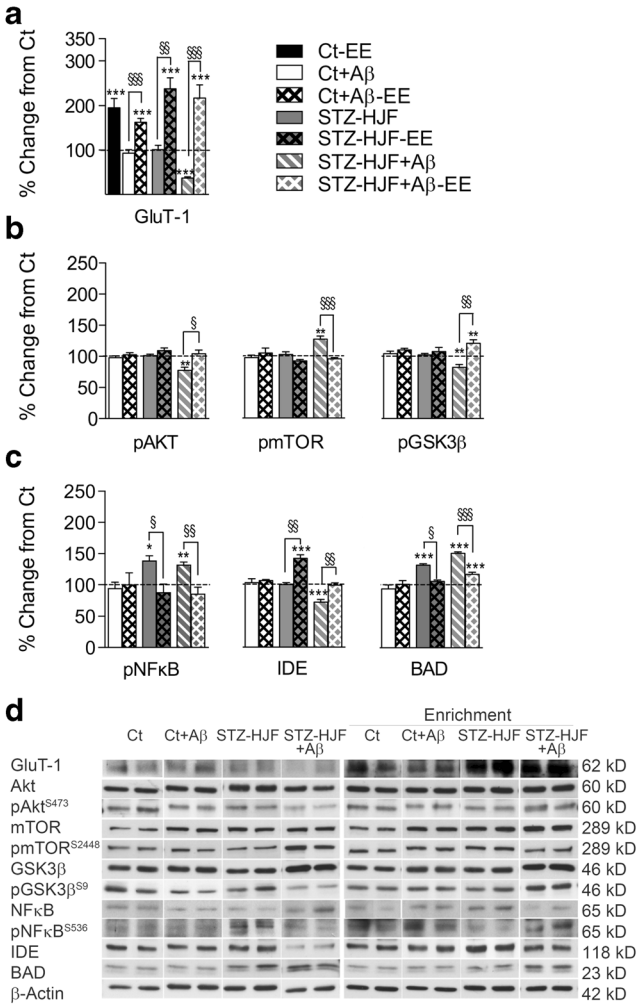

Fig. 11 Beneficial effect of environmental enrichment (EE) on proteins regulated by different treatments. Group means±SEM are represented for enriched groups: Ct-EE ($n = 4$); Ct + Aβ-EE ($n = 4$); STZ-HJF-EE ($n = 5$); STZ-HJF + Aβ-EE ($n = 5$) at W21 and Ct + Aβ ($n = 5$); STZ-HJF ($n = 5$); STZ-HJF + Aβ ($n = 5$). Histograms for corresponding non enriched groups are those represented in Figs. 8 and 9. **a** Shows changes specific to EE as it induced change in control rats. However, it also induced changes in all other groups. **b** Indicates changes induced by EE in STZ-HJF + Aβ treated rats. **c** Indicates change in both STZ-HFJ groups whether infused with Aβ or not. **d** Sample western blots (NB, representative blots for controls and non enriched groups are the same as those in Figs. 8 and 9). Asterisks indicate significant differences from control rats; *, $p < 0.05$; **, $p < 0.01$; ***, $p > 0.001$. § indicates where EE induced a significant difference compared with non-EE counter parts in each group; §, $p < 0.05$; §§, $p < 0.01$, §§§, $p < 0.001$

Aβ regulation of Gsk3β, APP and Beclin-1, and regulation of specific to STZ-HJF rats infused with Aβ and regulation of FoxO3 and mTOR induced by all treatments were immune to EE (Table 1, columns J, K; Fig. 11).

Discussion

The aim of these experiments was to determine whether a T2D phenotype could exacerbate deregulation of proteins in CA1 in or associated with IR/PI3K/Akt signalling induced by infusion of soluble Aβ alone. Our data show that when a soluble form of Aβ42 is infused in rats with a T2D profile, it induces long-lasting impairment in hippocampal-dependent memory and alteration of proteins in or associated with insulin/PI3K-Akt signalling in CA1. Treatment to induce T2D and infusion of Aβ alone had differential impact on memory processing and regulation of proteins. Finally, a mild form of environmental enrichment had a temporary beneficial effect on memory and could reverse some but not all changes in proteins. Although a number of the results we found find are subtle, it likely reflects changes induced in the early stages of AD and suggests they present a good case for some of the mechanisms by which T2D could pose a risk factor for AD.

Development of a T2D Phenotype

To our knowledge, this is the first time subdiabetogenic doses of STZ have been couple with human junk food to induce a characteristics of T2D. Mostly, STZ injections are coupled with calibrated high fat and/or high calorific diets as together they induce inflammation induced destruction of β pancreatic cells, impaired insulin secretion and stable hyperglycemia [37] and has been reported in numerous studies models [38]. Although consumption of HJF compared with calibrated obesity inducing diets inheritantly adds more variance into the results, what is lacking in calibrated diets is the presence of artificial additives such as preservatives, emulifiers, and colourants. Alone, food additives are capable of altering the

composition of microbiota and the gut brain axis [45]. Although rats fed HJF diet could not be considered obese compared with certain genetic models [46, 47], their weight is in the same range of a number of studies using cafeteria diet [48]. Moreover, it has been suggested that weight gain between 10 and 25% is an indicator of obesity [49, 50].

Coupling the HJF with STZ injections induced classic signs of a T2D phenotype that evolved with time where at the earlier stage rats displayed signs of hyperinsulinemia or insulin resistance but by the later stage they displayed hyperglycemia and much lower insulin levels that could suggest the start of β-pancreatic cell failure and a more advanced stage of T2D [51, 52] when certain patients require injections of insulin.

Memory Deficits Induced by Different Treatments

Apart from the pathology, memory deficits are what classically define AD and an increasing number of studies are showing that T2D is also associated with memory deficits [16]. In our experiments, we found that the T2D phenotype and infusion of Aβ alone induced different profiles of impairment, where T2D induced a mild but stable impairment and Aβ induced a more severe but temporary deficit. Together, however, the T2D phenotype prolonged the deficits induced by Aβ alone. To date, most experimental studies investigating memory impairment have demonstrated deficits in transgenic mice or with infusion of different species of Aβ; however, they have not repeatedly tested memory over a protracted period of time. Our results do find support in one study showing injections of oligomeric Aβ42 induced a temporary deficit in spatial memory that recovered [53] and another that showed injections of Aβ42 in rats made diabetic with STZ and high fat diet induced a more severe deficit in spatial memory compared with the treatments alone [54]. Importantly, a number of studies have shown high fat and/or high sucrose diet fed to AD transgenic mice accelerate cognitive deficits [55–61]; however, some show the deficits are independent of amyloid pathology [23, 52, 57]. This suggests that the dementia associated with AD is more likely triggered by multiple dysfunctional mechanisms independent of Aβ or associated with preaggregated species that may occur in parallel or at different stages of the disease as suggested by Herrup and colleagues [62, 63].

Environmental enrichment (EE) had a beneficial effect in all conditions; however, in control rats, this is dependent on demand on memory, and in those infused with Aβ, it unmasks a residual deficit at this longer retention delay. EE had a beneficial effect on performance in STZ-HJF treated rats either with or without infusion of Aβ; however, this was short lasting in both groups. Although EE has been shown to benefit memory in models of AD [40], its effects are subject to variables such as age at which animals are exposed, duration and strength of enrichment [64], and it is possible that extending the duration of EE or coupling it with exercise [65] may have a greater impact on STZ-HJF treatment with or without Aβ.

Regulation of the Akt Signalling Pathway and Associated Proteins in CA1 by Different Treatments

We examined basal expression and phosphorylation of proteins in CA1 as it is highly vulnerable to dysfunctions in early or prodromal stages [66–68]. All proteins were normalised to control/gel as % change. These values per group were then subsequently used for statistical analyses (see Table 1) and analysis of their regulation was conducted on two different levels. Firstly, we assessed whether protein regulation was specific to the combined STZ-HJF + Aβ treatment and whether this evolved with time; and secondly, how regulation of these proteins might contribute to dysfunction observed in AD vis a vis the existing literature. Most of the proteins we examined were altered by STZ-HJF + Aβ treatment, only expression of Akt, BAD and NFκB was not affected by any of the treatments. In general, at the late stage, STZ-HJF + Aβ induced increase in expression of total proteins and a decrease in the phosphorylated form. However, with Gsk3β, pGsk3β and pNFκB, the change evoked at the early timepoint was reversed with time and this may reflect time dependent biphasic [69].

At the most clear-cut level, we considered the late decrease in phosphorylation of Akt and expression of IDE, Beclin-1 and the increased expression of APP were specific to STZ-HJF treatment in conjunction with infusion of Aβ, as these proteins are not regulated at the early time point of 21 weeks, nor are they regulated by Aβ or STZ-HJF treatment alone at week 35 (Fig. 8a). We also considered the change in expression of mTOR and phosphorylation of mTOR and Gsk3β that was triggered at the early time point to be specific to the group in the absence of change induced by the treatments alone (Fig. 8b). Finally, the decrease in expression of GluT-1 was specific to this group, even though there was a similar decrease induced by Aβ alone at the early time point it was not sustained.

However, some proteins regulated by STZ-HJF + Aβ treatment were regulated in a similar manner by the treatments independently at either or both time points. This suggests the independent treatments may be the driving force behind that observed in the combined STZ-HJF + Aβ treatment, or that it may have a contributory effect. For example, the change in expression of BAD, and phosphorylation of NFκB observed with STZ-HJF + Aβ treatment, we attribute to the STZ-HJF treatment alone as the changes are identical with both groups

with STZ-HJF + Aβ treatment was also induce in a similar manner by infusion of Aβ alone at the early time point but was not sustained by the end of the experiment. Finally, the increase in expression of FoxO3, at both time points, and mTOR at the end of the experiment were induced by all 3 treatments independently and also by HJF alone, suggesting these proteins are highly susceptible to different effects that could be occurring simultaneously but in an independent manner.

The beneficial effect of EE in general impacted phosphorylation of proteins such as Akt, Gsk3β, mTOR and expression of proteins associated with insulin (IDE) regulation and glucose transport, important energy sources [70]. However, reversal of these effects by EE was not sufficient to maintain improvement in memory. Moreover, we might speculated that the lack of effect on mTOR, BAD and FoxO3 regulation may suggest they are resistant to EE as they can be mediated in parallel by different treatments independently.

Regulation of Proteins Induced by STZ-HJF + Aβ Treatment in Association with Dysfunction in AD

Our principle results show that STZ-HJF + Aβ treatment decreased phosphorylation of Akt at the late time point and was specific to this group. Regulation of Akt impacts downstream target proteins that are associated with hubs of protein interactions that mediate different functions disrupted in AD. The two most documented axes of regulation studied in AD are Akt-Gsk3β regulation as this has been implicated for the most part in tau phosphorylation and an increase in Aβ production [71] and Akt-mTOR that acts in concert with Akt-independent proteins to regulate autophagy [72], tau phosphorylation [73] and vasodilation and cerebral blood flow [10].

The increase in expression of Gsk3β was accompanied by a decrease in phosphorylation of the protein by Akt. Under normal conditions, Gsk3β is constitutively active and phosphorylation by Akt inhibits its activity. Our data therefore suggest that Gsk3β is in an active state. This is in agreement with some studies showing an increase in expression in the brains [24, 25] of AD patients and experimental studies [74], but not others [26, 75]. More specifically, our results agree with a single study showing more severe deregulation of Akt signalling in patients with AD and T2D than those with AD or T2D alone [76]. Over expression of GSK3β can hyperphosphorylate Tau [77] and mediate amyloidogenic processing of APP [78]. Although we did not measure tau or Aβ, we found increased expression of APP, which could indirectly support aberrant processing of APP potentially mediated via GSK3β. Furthermore, we found a decrease in IDE expression, a zinc metalloprotease involved in eliminating Aβ that has been observed in AD patients [79], AD transgenic mice [80] and transgenic mice fed high fat diet [58]. Our data therefore support the hypothesis suggesting that over activity of GSK3β can account for memory deficits, tau hyperphosphorylation and increased production of Aβ [81].

STZ-HJF + Aβ treatment also increased expression of mTOR and pmTOR compared with control rats, but phosphorylation was not induced directly by Akt at this specific site relative to expression of the protein. We also found the increase in expression of mTOR was regulated by all treatments, including STZ and HJF alone suggesting it is responsive to numerous signals that could include nutrient sensing, amino acids and stress signals [82]. Our results are in agreement with studies in AD showing an increase in both protein and gene expression [54, 83], and studies have shown reducing mTOR improves cognition, reduces Aβ and pTau and improves insulin signalling in an AD transgenic mouse [84, 85]. However, other studies have shown an increase in pmTOR at the same Akt site in the absence of change in expression levels in human AD brains and tissue [26, 75].

Regulation of mTOR is highly complex; it comprises 2 multiprotein complexes that have different phosphorylation sites [82] and could potentially undergo differential regulation at different stages during AD to impact different functions [86]. We cannot rule out the possibility that either the increase in pmTOR compared with controls is sufficient to exert an abnormal level of activation, that it is differentially regulated by the mTOR complexes [21], or other proteins such as S6K1 that phosphorylate this site that is susceptible to regulation by rapamycin and phorbol esters in an Akt-independent manner [87].

In conjunction with the increase in mTOR we also observed a significant decrease in expression levels of Beclin-1 specific to the STZ-HJF + Aβ group. Beclin-1 is a key activator of autophagy and works in concert with inhibition of mTOR to eliminate malformed proteins. A number of studies have shown autophagy is dysfunctional and expression of Beclin-1 is reduced in AD and T2D/obesity [13, 88–90], and overexpression of Beclin-1 protects against Aβ and increases in APP [72]. Thus, our results agree with those suggesting autophagic processes are disrupted in AD.

We also examined proteins regulated by Akt that are associated with inflammation (phosphorylation of NFκB) and apoptosis (BAD and FoxO3), common dysfunctional features in both AD [91–96]. In the absence of change in expression of the protein, we found hyperphosphorylation of NFκB at the late time point induced by STZ-HJF treatment regardless of whether rats were infused or not with Aβ, suggesting STZ-HJF treatment is responsible for the inflammatory response, which is not surprising as T2D is known to induce chronic low-grade inflammation, at least in the periphery [97, 98].

The increase in expression of both BAD and FoxO3 was regulated by all treatments, but in a different manner, where we attributed the increase in BAD to the T2D treatment and the increase in FoxO3 to both HJF alone and Aβ alone. Under normal conditions, phosphorylation of BAD and FoxO3 by Akt prevents activation of cell death mechanisms. Phosphorylation of BAD prevents it associating with proapoptotic proteins [98], whereas phosphorylation of FoxO3 sequesters it to the cytoplasm where it is maintained in an inactive state [see 99, 100]. The lack of a change in phosphorylation of BAD relative to the increased expression of the total protein suggests it is not phosphorylated by Akt and can be in an active state and potentially promote apoptosis.

The expression of total FoxO3 protein was also increased; however, we did not measure phosphorylation of the protein. Our result, however, is in keeping with other studies that show (a) an increase in FOXO3a mRNA in Alzheimer brains [101]; (b) inactivation of FoxO3a in the Tg2576 mouse model of AD attenuates AD neuropathology, whereas expression of constitutively active FoxO3a causally promotes amyloid processing [102], and (c) mice fed high fat diet induced a decrease in pAkt and an increase in FoxO3a in the nuclear compartment of neurons [103, 104].

Finally, we found a decrease in Glu-T1 in STZ-HJF + Aβ treated rats at the early time point that was exacerbated by the end of the experiment. We also found a decrease at the early time point induced by infusion of Aβ alone that was not long lasting, suggesting it may have a contributory effect to that observed with the combined STZ-HJF + Aβ treatment. Glu-T1 is the principle transporter of glucose across the BBB and reduction of uptake contributes to hypoglycaemia [105], a common feature of both AD and T2D [106]. However, it also maintains the cerebral architecture and disruption of its function can results in decreased blood flow and hypoperfusion as observed in AD patients and rodent models [107, 108]. Some evidence has shown that Aβ can impair the cerebral vasculature [109], suggesting that dysfunction in the BBB may be both a cause and a consequence of AD [9] (Fig. 12).

In conclusion, we found regulation of proteins associated with the promotion of amyloid and tau dysregulation and deregulation of functions that may be dependent or independent of early Aβ pathology. As our aim in this first step was to identify mechanisms associated with these dysfunctions in our model, we can only speculate how aberrantly regulated proteins we observe interact to induce dysfunctions based on the existing evidence (described in Fig. 13) and will require further experimentation. Nonetheless, our results show a number of important findings. (1) Coupling HJF with STZ has not yet been reported and this model shows classic signs of T2D and more closely resembles the human condition. (2) The T2D phenotype

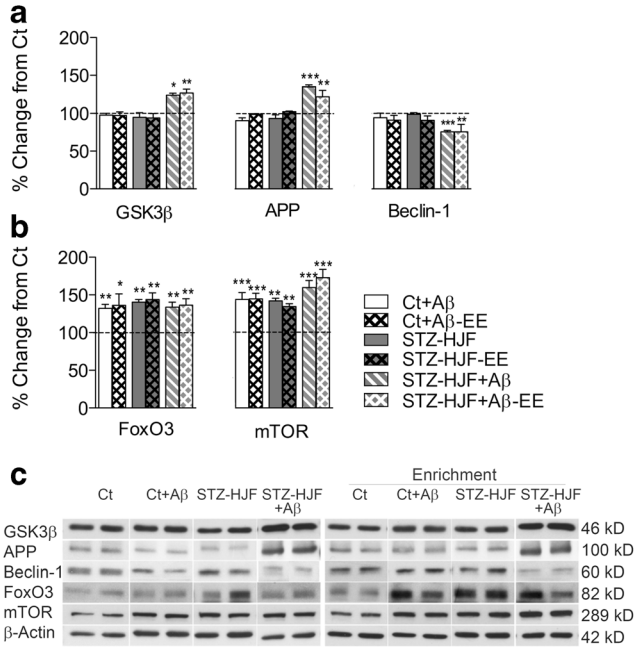

Fig. 12 Protein changes induced by different treatments that are resistant to environmental enrichment. Group means±SEM are described in the legend of Fig. 11. **a** Those specific to STZ-HJF + Aβ treatment. **b** Proteins regulated independently or in combination of different treatments. **c** Sample western blots (see explanation of bands from control and non enriched groups in Fig. 11 legend). Asterisks indicate significant differences from control rats; *, $p < 0.05$; **, $p < 0.01$; ***, $p > 0.001$. Data is represented as mean ± SEM. Week 35: Ct + Aβ

and infusion of Aβ alone induce different profiles of memory impairment, but together, suggests the temporary deficit induced by Aβ is prolonged on a T2D background, reinforcing T2D as a risk factor for AD at least in terms of a functional readout. (3) Regulation of proteins by different treatment is complex but suggest (a) the most robust deficits were observed with the combined T2D treatment with infusion of Aβ, suggesting for the majority of proteins we examined neither the T2D profile nor infusion of Aβ was sufficient alone to induce these changes. (b) The majority of changes in protein regulation were an increase in expression of the total protein with a lack or decrease in regulation by Akt. As Akt essentially puts a brake on activation of these proteins, it suggests that they are in an abnormally active state. (c) Certain proteins, notably expression of mTOR, BAD and FoxO3, are reactive to independent treatments and are resistant to beneficial effects of EE, suggesting they may be associated with key functions important in the early stages of AD that are promoted by T2D.

In total, our results support the growing hypotheses that suggest dysfunctional mechanisms implicated in mediating dementia in AD, are triggered by multiple 'hits' on functions essential for the support and maintenance of the neuronal milieu. They can be induced by amyloid

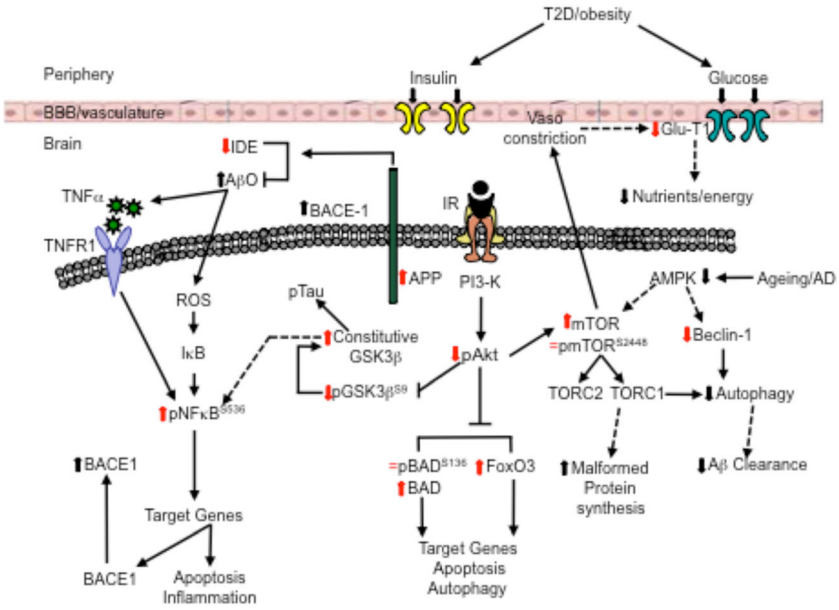

Fig. 13 Schema represents how the changes in proteins we observe may be incorporated in to known dysfunction associated with AD. Akt is a master regulator of a number of downstream proteins that themselves interact with hubs of protein complexes to elicit regulation of different functions. In general phosphorylation of these proteins by Akt is to inhibit their activity or to prevent their translocation to the nucleus. (1) In keeping with the decrease in phosphorylation of Akt is a decrease or lack of phosphorylation of Gsk3β, BAD and mTOR in relation to the increase in expression of the proteins. The lack of regulation of Gsk3β, can lead to accumulation of the constitutively active form of the protein. This has been shown to hyperphosphorylate Tau [73], but can also promote amyloidogenic process by promoting the liberation of Aβ from APP [77, 78]. More recently it has been shown Gsk3β can phosphorylate NFκB that leads to its translocation to the nucleus to activate genes associated with apoptosis and inflammation, but also transcribes BACE-1 [110]. (2) Increase in expression of APP proteins and decrease in expression of IDE suggests accumulation of AβO's that can bind to TNFα [111] and can interact with ROS [112] that in parallel can lead to translocation of NFκB also. (3) Phosphorylation of the BAD and FoxO's tether them in the cytoplasm, preventing them activating proapototic genes. The increase in expression of the 2 proteins suggests accumulation and at least with BAD it is not regulated by Akt, further suggesting they are in an active form. (4) Although expression of mTOR was increased, it was not phosphorylated by Akt. However, mTOR comprises 2 multiprotein complexes that can be phosphorylated by numerous imputs and contributes to numerous functions. Most relevant to AD and T2D, is that it is a biosensor of the nutritional/energy status and when activated it promotes protein translation and when inhibited it permits autophagic recycling or proteins. It is regulated in concert with Beclin that promotes autophagy and this is known to be dysfunctional in AD. AMPK is also an important sensor of nutrients and in non pathological conditions of low nutrient availability; it inhibits mTOR and activates Beclin-1. As the decrease in Glu-T1 would suggest a reduced level of nutrients, it should normally suggest AMPK activation of autophagy possibly via mTOR and Beclin-1 might be triggered. However AMPK levels are reduced in ageing and AD [113, 114], and as mTOR expression is increased and Beclin-1 decreased, it would suggest both AMPK and autophagy [115] are dysfunctional. The consequence of this may be an increase in malformed protein synthesis by mTOR and lack of clearance of these proteins and potentially Aβ species by autophagy. Recent evidence has also shown that aberrantly increased mTOR can induce vasoconstriction in neuronal vasculature and cerebral blood flow, that may contribute to reduced transport of glucose across the blood brain barrier (BBB), to perpetuate dysfunctional signalling of energy/nutrients necessary for normal neuronal functioning. Arrows indicate protein changes we find (red) and those previously reported in the literature (black). Solid lines represent reported relationship between protein interaction and dysfunction; broken lines represent speculated interaction and dysfunction in our experiments

dependent and independent mechanisms that would in turn depend on the dysfunctional mechanisms associated with different risk factors coupled with an age-dependent increase in soluble amyloid peptides.

Acknowledgements This work was supported by the Centre National de la Recherche Scientifique (CNRS, France); LECMA Vaincre Alzheimer, France (12702) to SD; the Hungarian Brain Research Programme 2.0 (2017-1.2.1-NKP-2017-00002) and Economy Development and Innovation Operative Programme (GINOP 2.3.2_15_2016_00038) to LF and ZB. KN was supported by LECMA funding and MS by the China Scholarship Council.

Author Contribution SD conceived and designed the research. MS, KN, NS and IY conducted the experiments. SD, BD, MS, KN and IY analysed data. IY and BD conducted all immunohistochemistry; LF and ZB produced and tested Aβ1-42 peptide. SD drafted the paper with contributions from MS and SL, and all authors read and approved the final manuscript.

Compliance with Ethical Standards

Conflict of Interest The authors declare that they have no conflict of interest

References

1. Ono K (2018) Alzheimer's disease as oligomeropathy. Neurochem Int 119:57–70. https://doi.org/10.1016/j.neuint.2017.08.010
2. Skaper SD (2012) Alzheimer's disease and amyloid: culprit or coincidence? Int Rev Neurobiol 102:277–316. https://doi.org/10.1016/B978-0-12-386986-9.00011-9
3. Holmes C, Boche D, Wilkinson D, Yadegarfar G, Hopkins V, Bayer A, Jones RW, Bullock R et al (2008) Long-term effects of Aβ 42 immunisation in Alzheimer's disease : follow-up of a randomised, placebo-controlled phase I trial. Lancet 372(9634):216–223. https://doi.org/10.1016/S0140-6736(08)61075-2
4. Driscoll I, Zhou Y, An Y, Sojkova J, Davatzikos C, Kraut MA, Ye W, Ferrucci L et al (2011) Lack of association between 11C-PiB and longitudinal brain atrophy in non-demented older individuals. Neurobiol Aging 32(12):2123–2130. https://doi.org/10.1016/j.neurobiolaging.2009.12.008
5. Maarouf CL, Daugs ID, Kokjohn TA, Walker DG, Hunter JM, Kruchowsky JC, Woltjer R, Kaye J et al (2011) Alzheimer's disease and non-demented high pathology control nonagenarians: comparing and contrasting the biochemistry of cognitively successful aging. PLoS One 6(11):e27291. https://doi.org/10.1371/journal.pone.0027291
6. Atwood CS, Bowen RL (2015) A unified hypothesis of early-and late-onset Alzheimer's disease pathogenesis. J Alzheimers Dis 47(1):33–47. https://doi.org/10.3233/JAD-143210
7. De Felice FG, Lourenco ML, Ferreira ST (2014) How does brain insulin resistance develop in Alzheimer's disease? Alzheimers Dement 10(1 suppl):S26–S32. https://doi.org/10.1016/j.jalz.2013.12.004
8. de Wilde MC, Vellas B, Girault E, Yavuz AC, Sijben JW (2017) Lower brain and blood nutrient status in Alzheimer's disease: results from meta-analyses. Alzheimers Dement 3(3):416–431. https://doi.org/10.1016/j.trci.2017.06.002
9. Erickson MA, Banks WA (2013) Blood-brain barrier dysfunction as a cause and consequence of Alzheimer's disease. J Cereb Blood Flow Metab 33(10):1500–1513. https://doi.org/10.1038/jcbfm.2013.135
10. Galvan V, Hart MJ (2016) Vascular mTOR-dependent mechanisms linking the control of aging to Alzheimer's disease. Biochim Biophys Acta 1862:992–1007. https://doi.org/10.1016/j.bbadis.2015.11.010
11. Gerakis Y, Hetz C (2018) Emerging roles of ER stress in the etiology and pathogenesis of Alzheimer's disease. FEBS J 285(6):995–1011. https://doi.org/10.1111/febs.14332
12. Gibas KJ (2017) The starving brain: Overfed meets undernourished in the pathology of mild cognitive impairment (MCI) and Alzheimer's disease (AD). Neurochem Int 110:57–68. https://doi.org/10.1016/j.neuint.2017.09.004
13. Uddin S, Stachowiak A, Al Mamun A, Tzvetkov NT, Takeda S, Atanasov AG, Bergantin LB, Abdel-Daim MM et al (2018) Autophagy and Alzheimer's disease: from molecular mechanisms to therapeutic implications. Front Aging Neurosci. https://doi.org/10.3389/fnagi.2018.00004
14. Yin F, Sancheti H, Patil I, Cadenas E (2016) Energy metabolism and inflammation in brain aging and Alzheimer's disease. Free Radic Biol Med 100:108–122. https://doi.org/10.1016/j.freeradbiomed.2012.04.200
15. Paul KC, Jerrett M, Ritz B (2018) Type 2 diabetes mellitus and Alzheimer's disease: overlapping biologic mechanisms and environmental risk factors. Curr Environ Health Rep 5(1):1–15. https://doi.org/10.1007/s40572-018-0176-1
16. Gorska-Ciebiada M, Saryusz-Wolska M, Ciebiada M, Loba J (2014) Mild cognitive impairment and depressive symptoms in elderly patients with diabetes: prevalence, risk factors, and comorbidity. J Diabetes Res 2014:1–7. https://doi.org/10.1155/2014/179648
17. Jack CR, Knopman DS, Jagust WJ, Shaw LM, Aisen PS, Weiner MW, Petersen RC, Trojanowski JQ (2010) Hypothetical model of dynamic biomarkers of the Alzheimer's pathological cascade. Lancet Neurol 9(1):119–128. https://doi.org/10.1016/S1474-4422(09)70299-6
18. Leitner DR, Frühbeck G, Yumuk V, Schindler K, Micic D, Woodward E, Toplak H (2017) Obesity and type 2 diabetes: two diseases with a need for combined treatment strategies - EASO can lead the way. Obes Facts 10(5):483–492. https://doi.org/10.1159/000480525
19. Templeman NM, Skovso S, Page MM, Lim GE, Johnson JD (2017) A causal role for hyperinsulinemia in obesity. J Endocrinol 232(3):R173–R183. https://doi.org/10.1530/JOE-16-0449
20. Daulatzai MA (2017) Cerebral hypoperfusion and glucose hypometabolism: key pathophysiological modulators promote neurodegeneration, cognitive impairment, and Alzheimer's disease. J Neurosci Res 95(4):943–972. https://doi.org/10.1002/jnr.23777
21. Vieira MNN, Lima-Filho RAS, De Felice FG (2018) Connecting Alzheimer's disease to diabetes: underlying mechanisms and potential therapeutic targets. Neuropharmacol 136(Pt B):160–171. https://doi.org/10.1016/2017.11.014
22. Verdile G, Fuller SJ, Martins RN (2015) The role of type 2 diabetes in neurodegeneration. Neurobiol Dis 84:22–38. https://doi.org/10.1016/j.nbd.2015.04.008
23. Pruzin JJ, Nelson PT, Abner EL, Arvanitakis Z (2018) Relationship of type 2 diabetes to human brain pathology. Neuropathol Appl Neurobiol 44(4):347–362. https://doi.org/10.1111/nan.12476
24. Blalock EM, Geddes JW, Chen KC, Porter NM, Markesbery WR, Landfield PW (2004) Incipient Alzheimer's disease: microarray correlation analyses reveal major transcriptional and tumor suppressor responses. Proc Natl Acad Sci 101(7):2173–2178. https://doi.org/10.1073/pnas.0308512100
25. Steen E, Terry BM, Rivera EJ, Cannon JL, Neely TR, Tavares R, Xu XJ, Wands JR et al (2005) Impaired insulin and insulin-like growth factor expression and signaling mechanisms in Alzheimer's disease—is this type 3 diabetes? J Alzheimers Dis 7(1):63–80. https://doi.org/10.3233/JAD-2005-7107
26. Griffin RJ, Moloney A, Kelliher M, Johnston JA, Ravid R, Dockery P, O'Connor R, O'Neill C (2005) Activation of Akt/PKB, increased phosphorylation of Akt substrates and loss and altered distribution of Akt and PTEN are features of Alzheimer's disease pathology. J Neurochem 93(1):105–117. https://doi.org/10.1111/j.1471-4159.2004.02949.x
27. Busquets O, Ettcheto M, Pallàs M, Beas-Zarate C, Verdaguer E, Auladell C, Folch J, Camins A (2017) Long-term exposition to a high fat diet favors the appearance of β-amyloid depositions in the brain of C57BL/6J mice. A potential model of sporadic Alzheimer's disease. Mech Ageing Dev 162:38–45. https://doi.org/10.1016/j.mad.2016.11.002
28. Salas IH, Weerasekera A, Ahmed T, Callaerts-Vegh Z, Himmelreich U, D'Hooge R, Balschun D, Saido TC et al (2018) High fat diet treatment impairs hippocampal long term

potentiation without alterations of the core neuropathological features of Alzheimer's disease. Neurobiol Dis 113:82–96. https://doi.org/10.1016/j.nbd.2018.02.001
29. Carvalho C, Cardoso S, Correia SC, Santos RX, Santos MS, Baldeiras I, Oliveira CR, Moreira PI (2012) Metabolic alterations induced by sucrose intake and Alzheimer's disease promotes similar brain mitochondrial abnormalities. Diabetes 61(5):1234–1242. https://doi.org/10.1016/j.nbd.2018.02.001
30. Hiltunen M, Khandelwal VKM, Yaluri N, Tiilikainen T, Tusa M, Koivisto H, Krzisch M, Vepsäläinen S et al (2012) Contribution of genetic and dietary insulin resistance to Alzheimer phenotype in APP/PS1 transgenic mice. J Cell Mol Med 16(6):1206–1222. https://doi.org/10.1111/j.1582-4934.2011.01384.x
31. Ramos-Rodriguez JJ, Spires-Jones T, Pooler AM, Lechuga-Sancho AM, Bacskai BJ, Garcia-Alloza M (2017) Progressive neuronal pathology and synaptic loss induced by prediabetes and type 2 diabetes in a mouse model of Alzheimer's disease. Mol Neurobiol 54(5):3428–3438. https://doi.org/10.1007/s12035-016-9921-3
32. Alagiakrishnan K, Sankaralingam S, Ghosh M, Mereu L, Senior P (2013) Antidiabetic drugs and their potential role in treating mild cognitive impairment and Alzheimer's disease. Discov Med 16(90):277–286
33. Holscher C (2018) Novel dual GLP-1/GIP receptor agonists show neuroprotective effects in Alzheimer's and Parkinson's diease models. Neuropharmacol 136(PtB):251–259. https://doi.org/10.1016/j.neuropham.2018.01.040
34. Grieb P (2016) Intracerebroventricular Streptozotocin injections as a model of Alzheimer's disease: in search of a relevant mechanism. Mol Neurobiol 53:1741–1752. https://doi.org/10.1007/s12035-015-9132-3
35. Kamat PK, Kalani A, Rai S, Tota SK, Kumar A, Ahmad AS (2016) Streptozotocin Intracerebroventricular-induced neurotoxicity and brain insulin resistance: a therapeutic intervention for treatment of sporadic Alzheimer's disease (sAD)-like pathology. Mol Neurobiol 53(7):4548–4562. https://doi.org/10.1007/s12035-015-9384-y
36. Chami B, Steel AJ, De La Monte SM, Sutherland GT (2016) The rise and fall of insulin signaling in Alzheimer's disease. Metab Brain Dis 31(3):497–515. https://doi.org/10.1007/s11011-016-9806-1
37. Zhang M, Lv X-Y, Xu Z-G, Chen L (2008) The characterization of highfat diet and multiple low-dow Streptozotocin induced type 2 diabetes rat model. Exp Diabet Res 704045. https://doi.org/10.1155/2008/704045.
38. Skovso S (2014) Modeling type 2 diabetes in rats using high fat diet and streptozotocin. J Diabetes Investig 5(4):349–358. https://doi.org/10.1111/jdi.12235
39. Ohline SM, Abraham WC (2018) Environmental enrichment effects on synaptic and cellular physiology of hippocampal neurons. Neuropharmacol. https://doi.org/10.1016/j.neuropharm.2018.04.007
40. Costa DA, Cracchiolo JR, Bachstetter AD, Hughes TF, Bales KR, Paul SM, Mervis RF, Arendash GW et al (2007) Enrichment improves cognition in AD mice by amyloid-related and unrelated mechanisms. Neurobiol Aging 28(6):831–844. https://doi.org/10.1016/j.neurobiolaging.2006.04.009
41. Bozso Z, Penke B, Simon D, Laczkó I, Juhász G, Szegedi V, Kasza A, Soós K et al (2010) Controlled in situ preparation of a beta(1-42) oligomers from the isopeptide "iso-A beta(1-42)", physicochemical and biological characterization. Peptides 31(2):248–256. https://doi.org/10.1016/j.peptides.2009.12.001
42. Bruel-Jungerman E, Laroche S, Rampon C (2005) New neurons in the dentate gyrus are involved in the expression of enhanced long-term memory following environmental enrichment. Eur J Neurosci 21(2):513–521. https://doi.org/10.1111/j.1460-9568.2005.03875.x
43. Davis S, Vanhoutte P, Pages C, Caboche J, Laroche S (2000) The MAPK/ERK cascade targets both Elk-1 and cAMP response element-binding protein to control long-term potentiation-dependent gene expression in the dentate gyrus in vivo. J Neurosci 20(12):4563–4572. https://doi.org/10.1523/JNEUROSCI.20-12-04563.2000
44. Kayed R, Head E, Sarsoza F, Saing T, Cotman CW, Necula M, Margol L, Wu J et al (2007) Fibril specific, conformation dependent antibodies recognize a generic epitope common to amyloid fibrils and fibrillar oligomers that is absent in prefibrillar oligomers. Mol Neurodegener 26:2–18. https://doi.org/10.1186/1750-1326-2-18
45. Holder MK, Chassaing B (2018) Impact of food additives on the gut-brain axis. Physiol Behav 192:173–176. https://doi.org/10.1016/j.physbeh.2018.02.025
46. Bray GA (1977) The Zucker-fatty rat: a review. Fed Proc 36(2):148–153
47. Harishankar N, Vajreswari A, Giridharan NV (2011) WNIN/GR-Ob an insulin-resistant obese rat model from inbred WNIN strain. Indian J Med Res 134:320–329
48. Shafat A, Murray B, Rumsey D (2009) Energy density in cafeteria diet induced hyperphagia in the rat. Appetite 52(1):34–38. https://doi.org/10.1016/j.appet.2008.07.004
49. Levin BE, Dunn-Meynell AA (2002) Reduced central leptin sensitivity in rats with diet-induced obesity. Am J Phys Regul Integr Comp Phys 283(5):R941–R948. https://doi.org/10.1152/ajpregu.00245.2002
50. Woods SC, Seeley RJ, Rushing PA, D'Alessio D, Tso P (2003) A controlled high-fat diet induces an obese syndrome in rats. J Nutr 133(4):1081–1087. https://doi.org/10.1093/jn/133.4.1081
51. Leahy JL (2005) Pathogenesis of type 2 diabetes mellitus. Arch Med Res 36(3):197–209. https://doi.org/10.1016/j.arcmed.2005.01.003
52. Alejandro EU, Gregg B, Blandino-Rosano M, Cras-Méneur C, Bernal-Mizrachi E (2014) Natural history of beta-cell adaptation and failure in type 2 diabetes. Mol Asp Med 42:19–41. https://doi.org/10.1016/j.mam.2014.12.002
53. Wong RS, Cechetto DF, Whitehead SN (2016) Assessing the effects of acute amyloid β oligomer exposure in the rat. Int J Mol Sci 17(9):1390–1403. https://doi.org/10.3390/ijms17091390
54. Ma YQ, Wu DK, Liu JK (2013) mTOR and tau phosphorylated proteins in the hippocampal tissue of rats with type 2 diabetes and Alzheimer's disease. Mol Med Rep 7(2):623–627. https://doi.org/10.3892/mmr.2012.1186
55. Knight EM, Martins IVA, Gümüsgöz S, Allan SM, Lawrence CB (2014) High-fat diet-induced memory impairment in triple-transgenic Alzheimer's disease (3xTgAD) mice is independent of changes in amyloid and tau pathology. Neurobiol Aging 35(8):1821–1832. https://doi.org/10.1016/j.neurobiolaging.2014.02.010
56. Ho L, Qin W, Pompl PN, Xiang Z, Wang J, Zhao Z, Peng Y, Cambareri G et al (2004) Diet induced insulin resistance promotes amyloidosis in a transgenic mouse model of Alzheimer's disease. FASEB J 18(7):902–924. https://doi.org/10.1096/fj.03-0978fje
57. Cao D, Lu H, Lewis TL, Li L (2007) Intake of sucrose-sweetened water induces insulin resistance and exacerbates memory deficits and amyloidosis in a transgenic mouse model of Alzheimer disease. J Biol Chem 282(50):36275–36282. https://doi.org/10.1074/jbc.M703561200
58. Vandal M, White PJ, Tremblay C, St-Amour I, Chevrier G, Emond V, Lefrancois D, Virgili J et al (2014) Insulin reverses the high-fat diet-induced brain Aβ and improves memory in an animal model of Alzheimer's disease. Diabetes 63(12):4291–4301. https://doi.org/10.2337/db14-0375

59. Fitz NF, Cronican A, Pham T, Fogg A, Fauq AH, Chapman R, Lefterov I, Koldamova R (2010) Liver X receptor agonist treatment ameliorates amyloid pathology and memory deficits caused by high-fat diet in APP23 mice. J Neurosci 30(20):6862–6872. https://doi.org/10.1523/JNEUROSCI.1051-10.2010
60. Herculano B, Tamura M, Ohba A, Shimatani M, Kutsuna N, Hisatsune T (2013) β-Alanyl-L-histidine rescues cognitive deficits caused by feeding a high fat diet in a transgenic mouse model of Alzheimer's disease. J Alzheimers Dis 33(4):983–997. https://doi.org/10.3233/JAD-2012-121324
61. Maesako M, Uemura K, Kubota M, Kuzuya A, Sasaki K, Asada M, Watanabe K, Hayashida N et al (2012) Environmental enrichment ameliorated high-fat diet-induced Aβ deposition and memory deficit in APP transgenic mice. Neurobiol Aging 33(5): 1011.e11–1011.e23. https://doi.org/10.1016/j.neurobiolaging.2011.10.028
62. Herrup K (2010) Reimagining Alzheimer's disease—an age-based hypothesis. J Neurosci 30(50):16755–16762. https://doi.org/10.1523/JNEUROSCI.4521-10.2010
63. Herrup K, Carrillo MC, Schenk D, Cacace A, DeSanti S, Fremeau RF, Bhat R, Glicksman M et al (2013) Beyond amyloid: getting real about nonamyloid targets in Alzheimer's disease. Alzheimers Dement 9(4):452–458. https://doi.org/10.1016/j.jalz.2013.01.017
64. Redolat R, Mesa-Gresa P (2012) Potential benefits and limitations of enriched environments and cognitive activity on age-related behavioural decline. Curr Top Behav Neurosci 10:293–316. https://doi.org/10.1007/7854_2011_134
65. Prado Lima MG, Schimidt HL, Garcia A, Daré LR, Carpes FP, Izquierdo I, Mello-Carpes PB (2018) Environmental enrichment and expercise are better than social enrichment to reduce memory deficits in amyloid beta neurotoxicity. Proc Natl Acad Sci 115(10): E2403–E2409. https://doi.org/10.1073/pnas.1718435115
66. La Joie R, Perrotin A, de la Sayette V, Egret S, Doeuvre L; Belliard S, Eustache F, Desgranges B, Chételat G (2013) Hippocampal subfield volumetry in mild cognitive impairment, Alzheimer's disease and semantic dementia. Neuroimage Clin 3:155–162. https://doi.org/10.1016/j.nicl.2013.08.007
67. Counts SE, Alldred MJ, Che S, Ginsberg SD, Mufson EJ (2013) Synaptic gene dysregulation within hippocampal CA1 pyramidal neurons in mild cognitive impairment. Neuropharmacology 79: 172–179. https://doi.org/10.1016/j.neuropharm.2013.10.018
68. Masurkar AV (2018) Towards a circuit-level understanding of hippocampal CA1 dysfunction in Alzheimer's disease across anatomical axes. J Alzheimers Dis Parkinsonism 8(1).
69. Jimenez S, Torres M, Vizuete M, Sanchez-Varo R, Sanchez-Mejias E, Trujillo-Estrada L, Carmona-Cuenca I, Caballero C et al (2011) Age-dependent accumulation of soluble amyloid beta (Aβ) oligomers reverses the neuroprotective effect of soluble amyloid precursor protein-α (sAPPα) by modulating phosphatidylinositol 3-kinase (PI3K)/Akt-GSK-3β pathway in Alzheimer mouse model. J Biol Chem 286:18414–18425
70. Qutub AA, Hunt CA (2005) Glucose transport to the brain: a systems model. Brain Res Brain Res Rev 49(3):595–617. https://doi.org/10.1016/j.brainresrev.2005.03.002
71. Martin L, Latypova X, Wilson CM, Magnaudeix A, Perrin A-L, Yardin C, Terro F (2013) Tau protein kinases: involvement in Alzheimer's Disease. Ageing Res Rev 12(1):289–309. https://doi.org/10.1016/j.arr.2012.06.003
72. Jaeger PA, Wyss-Coray T (2010) Beclin 1 complex in autophagy and Alzheimer disease. Arch Neurol 67(10):1181–1184. https://doi.org/10.1001/archneurol.2010.258
73. Caccamo A, Magr A, Medina DX, Silva AJ, Wisely EV, Manuel FL, Oddo S (2013) mTOR regulates tau phosphorylation and degradation: implications for Alzheimer's disease and other tauopathies. Aging Cell 12(3):370–380. https://doi.org/10.1111/acel.12057
74. Farr SA, Ripley JL, Sultana R, Zhang Z, Niehoff ML, Platt TL, Murphy MP, Morely JE et al (2014) Antisense oligonucleotide against GSK-3β in brain of SAMP8 mice improves learning and memory and decreases oxidative stress: Involvement of transcription factor Nrf2 and implications for Alzheimer disease. Free Radic Biol Med 67:387–395. https://doi.org/10.1016/j.freeradbiomed.2013.11.014
75. Tramutola A, Triplett JC, Di Domenico F, Niedowicz DM, Murphy MP, Coccia R, Perluigi M, Butterfield DA (2015) Alteration of mTOR signalling occurs early in the progression of Alzheimer disease (AD): analysis of brain from subjects with pre-clinical AD, amnestic mild cognitive impairment and late-stage AD. J Neurochem 133(5):739–749. https://doi.org/10.1111/jnc.13037
76. Liu Y, Grundke-Iqbal FLI, Gong KI, Gong C-X (2011) Deficient brain insulin signalling pathway in Alzheimer's disease and diabetes. J Pathol 225(1):54–62. https://doi.org/10.1002/path.2912
77. Maqbool M, Mobashir M, Hoda N (2016) Pivital role of glycogen synthase kinase-3: a therapeutic target for Alzheimer's disease. Eur J Med Chem 107:63–81. https://doi.org/10.1016/j.emech.2015.10.018
78. Lee YS, Chow WNV, Lau K-F (2017) Phosphorylation of FE65 at threonine 579 by GSK3β stimulates amyloid precursor protein processing. Sci Rep 7(1):12456. https://doi.org/10.1038/s41598-017-12334-2
79. Qiu WQ, Folstein MF (2006) Insulin, insulin-degrading enzyme and amyloid-beta peptide in Alzheimer's disease: review and hypothesis. Neurobiol Aging 27(2):190–198
80. Vepsäläinen S, Hiltunen M, Helisalmi S, Wang J, van Groen T, Tanila H, Soininen H (2008) Increased expression of Abeta degrading enzyme IDE in the cortex of transgenic mice with Alzheimer's disease-like neuropathology. Neurosci Lett 438(2): 216–220. https://doi.org/10.1016/j.neulet.2008.04.025
81. Hooper C, Killick R, Lovestone S (2008) The GSK3 hypothesis of Alzheimer's disease. J Neurochem 104(6):1433–1439. https://doi.org/10.1111/j.1471-4159.2007.05194.x
82. Huang K, Fingar DC (2014) Growing knowledge of the mTOR signaling network. Semin Cell Dev Biol 36:79–90. https://doi.org/10.1016/j.semcdb.2014.09.011
83. Sun YX, Ji X, Mao X, Xie L, Jia J, Galvan V, Greenberg DA, Jin K (2014) Differential activation of mTOR complex 1 signaling in human brain with mild to severe Alzheimer's disease. J Alzheimers Dis 38(2):437–444. https://doi.org/10.3233/JAD-131124
84. Spilman P, Podlutskaya N, Hart MJ, Debnath J, Gorostiza O, Bredensen D, Richardson A, Strong R et al (2010) Inhibition of mTOR by rapamycin abolishes cognitive deficits and reduces amyloid-β levels in a mouse model of Alzheimer's disease. PLoS One 5(4):e9979. https://doi.org/10.1371/journal.pone.0009979
85. Caccamo A, Belfiore R, Oddo S (2018) Genetically reducing mTOR signaling rescues central insulin dysregulation in a mouse model of Alzheimer's disease. Neurobiol Aging 68:59–67. https://doi.org/10.1016/j.neurobiolaging.2018.03.032
86. Caccamo A, De Pinto V, Messina A, Branca C, Oddo S (2014) Genetic reduction of mammalian target of rapamycin ameliorates Alzheimer's disease-like cognitive and pathological deficits by restoring hippocampal gene expression signature. J Neurosci 34(23):7988–7998. https://doi.org/10.1523/JNEUROSCI.0777-14.2014
87. Holz MK, Blenis J (2005) Identification of S6 kinase 1 as a novel mammalian target of rapamycin (mTOR)-phosphorylating kinase. J Biol Chem 280(28):26089–26093. https://doi.org/10.1074/jbc.M504045200
88. François A, Rioux-Bilan A, Quellard N, Fernandez B, Janet T, Chassaing D, Paccalin M, Terro F et al (2014) Longitudinal

follow-up of autophagy and inflammation in brain of APPswePS1dE9 transgenic mice. J Neuroinflammation 11:139. https://doi.org/10.1186/s12974-014-0139
89. Zhang Y, Sowers JR, Ren J (2018) Targeting autophagy in obesity: from pathophysiology to management. Nat Rev Endocrinol 14(6): 356–376. https://doi.org/10.1038/s41574-018-0009-1
90. Kim J, Lim YM, Lee MS (2018) The role of autophagy in systemic metabolism and human-type diabetes. Mol Cells 41(1):11–17. https://doi.org/10.14348/molcells.2018.2228
91. Skaper SD, Facci L, Zusso M, Giusti P (2018) An inflammation-centric view of neurological disease: beyond the neuron. Front Cell Neurosci 12:72. https://doi.org/10.3389/fncel.2018.00072
92. Pompl PN, Yemul S, Xiang Z, Ho L, Haroutunian V, Purohit D, Mohs R, Pasinetti GM (2003) Caspase gene expression in the brain as a function of the clinical progression of Alzheimer disease. Arch Neurol 60(3):369–376. https://doi.org/10.1001/archneur.60.3.369
93. Obulesu M, Lakshmi MJ (2014) Apoptosis in Alzheimer's disease: an understanding of the physiology, pathology and therapeutic avenues. Neurochem Res 39(12):2301–2312. https://doi.org/10.1007/s11064-014-1454-4
94. Maiese K (2008) Triple play: promoting neurovascular longevity with nicotinamide, wnt and erythropoietin in diabetes mellitus. Biomed Pharmacother 62(4):218–232. https://doi.org/10.1016/j.biopha.2008.01.009
95. van Dijk G, van Heijningen S, Reijne AC, Nyakas C, van der Zee EA, Eisel UL (2015) Integrative neurobiology of metabolic diseases, neuroinflammation, and neurodegeneration. Front Neurosci 9:173. https://doi.org/10.3389/fnins.2015.00173
96. Ljubicic S, Polak K, Fu A, Wiwczar J, Szlyk B, Chang Y, Alvez-Perez JC, Bird GH et al (2015) Phospho-BAD BH3 mimicry protects β cell and restores functional β cell mass in diabetes. Cell Rep 10(4):497–504. https://doi.org/10.1016/j.celrep.2014.12.056
97. van Greevenbroek MMJ, Schalkwijk CG, Stehouwer CDA (2013) Obesity-associated low-grade inflammation in type 2 diabetes mellitus: causes and consequences. Neth J Med 71(4):174–187
98. Datta SR, Dudek H, Tao X, Masters S, Fu H, Gotoh Y, Greenberg ME (1997) Akt phosphorylation of BAD couples signals to the cell-intrinsic death machinery. Cell 91:231–241
99. Leong ML, Maiyar AC, Kim B, O'Keeffe BA, Firestone GL (2003) Expression of the serum- and glucocorticoid-inducible protein kinase, Sgk, is a cell survival response to multiple types of environmental stress stimuli in mammary epithelial cells. J Biol Chem 278(8):5871–5882. https://doi.org/10.1074/jbc.M211649200
100. Shi C, Viccaro K, Lee H-G, Sha K (2016) Cdk5-Foxo3 axis: initially neuroprotective, eventually neurodegenerative in Alzheimer's disease models. J Cell Sci 129:1815–1830. https://doi.org/10.1242/jcs.185009
101. Qin W, Zhao W, Ho L, Wang J, Walsh K, Gandy S, Pasinetti GM (2009) Regulation of forkhead transcription factor FoxO3a contributes to calorie restriction-induced prevention of Alzheimer's disease-type amyloid neuropathology and spatial memory deterioration. Ann N Y Acad Sci 1147:335–347. https://doi.org/10.1196/annals.1427.024
102. Qin W, Zhao W, Ho L, Wang J, Walsh K, Gandy S, Pasinetti GM (2008) Regulation of forkhead transcription factor FoxO3a contributes to calorie restriction-induced prevention of Alzheimer's disease-type amyloid neuropathology and spatial memory deterioration. Ann N Y Acad Sci 1147:335–347. https://doi.org/10.1196/annals.1427.024
103. Nuzzo D, Picone P, Baldassano S, Caruana L, Messina E, Marino Gammazza A, Cappello F, Mulè F et al (2015) Insulin resistance as common molecular denominator linking obesity to Alzheimer's disease. Curr Alzheimer Res 12(8):723–35.94
104. Martins R, Lithgow GJ, Link W (2016) Long live FOXO: unravelling the role of FOXO proteins in ageing and longevity. Aging Cell 15(2):196–207. https://doi.org/10.1111/acel.12427
105. Shah K, DeSilva S, Abbruscato T (2012) The role of glucose transporters in brain disease: diabetes and Alzheimer's disease. Int J Mol Sci 13(10):12629–12655. https://doi.org/10.3390/ijms131012629
106. Meneilly GS, Tessier DM (2016) Diabetes, dementia and hypoglycemia. Can J Diabetes 40(1):73–76. https://doi.org/10.1016/j.jcjd.2015.09.006
107. Sato N, Morishita R (2013) Roles of vascular and metabolic components in cognitive dysfunction of Alzheimer's disease: short- and long-term modification by non-genetic risk factors. Front Aging Neurosci 5(64). https://doi.org/10.3389/fnagi.2013.00064
108. Montagne A, Zhao Z, Zlokovic BV (2017) Alzheimer's disease: a matter of blood-brain barrier dysfunction? J Exp Med 214(11): 3151–3169. https://doi.org/10.1084/jem.20171406
109. Niwa K, Younkin L, Ebeling C, Turner SK, Westaway D, Younkin S, Hsiao-Ashe K, Carlson GA et al (2000) Aβ-40-related reduction in functional hyperemia in mouse neocortex during somatosensory activation. Proc Natl Acad Sci USA 97(17):9735–9740. https://doi.org/10.1073/pnas.97.17.9735
110. Ly PTT, Wu Y, Zou H, Wang R, Zhou W, Kinoshita A, Zhang M, Yang Y et al (2013) Inhibition of GSK3β-mediated BACE1 expression reduces Alzheimer-associated phenotypes. J Clin Invest 123(1):224–235. https://doi.org/10.1172/JCI64516
111. Decourt B, Lahiri DK, Sabbagh MN (2017) Targeting tumor necrosis factor alpha for Alzheimer's disease. Curr Alzheimer Res 14(4): 412–425. https://doi.org/10.2174/1567205013666160930110551
112. Ahmad W, Ijaz B, Shabbiri K, Ahmed F, Rehman S (2017) Oxidative toxicity in diabetes and Alzheimer's disease: mechanisms behind ROS/RNS generation. J Biomed Sci 24(1):76. https://doi.org/10.1186/s12929-017-0379-z
113. Salminen A, Kaarniranta K, Haapasalo A, Soininen H, Hiltunen M (2011) AMP-activated protein kinase: a potential player in Alzheimer's disease. J Neurochem 118(4):460–474. https://doi.org/10.1111/j.1471-4159.2011.07331.x
114. Cai Z, Yan LJ, Li K, Quazi SH, Zhao B (2012) Roles of AMP-activated protein kinase in Alzheimer's disease. Neuromol Med 14(1):1–14. https://doi.org/10.1007/s12017-012-8173-2
115. Metaxakis A, Ploumi C, Tavernarakis N (2018) Autophagy in age-associated neurodegeneration. Cells 7(5):E37. https://doi.org/10.1186/s12929-017-0379-z